Office of Naval Research

Contract N50RI-76 • Task Order No.1 • NR-078-011

A UHF IMPEDANCE BRIDGE FOR SHIELDED TWO-WIRE LINES

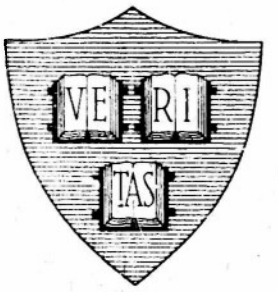

By

Edgar W. Matthews, Jr.

March 10, 1954

Technical Report No. 184

Cruft Laboratory
Harvard University
Cambridge, Massachusetts

JOINT SERVICE CONTRACT (Navy, SigC, AF) N5ori-07601 & 28

CRUFT LABORATORY, HARVARD UNIVERSITY

Tech Rpt 184 dd 10 Mar 54 "A UHF Impedance Bridge for Shielded Two-Wire Lines"

SCEL DISTRIBUTION

No Cys	To
1	Chief, Radar Dev Br.ESL
1	Chief GM Instru Br.ESL
1	Chief, Radar Systems Br.ESL
1	Chief, App Physics Br.ESL
1	Chief, Thermionics Br.ESL
1	Chief, Met Br.ESL
1	Chief, Math & Met Br.ESL
1	Chief, Solid State Devices Br.ESL
1	Chief, Special Projects Br.ESL
1	Chief, C/M Eqt Br.ESL
1	C/M Div. Attn: Mr. J.J. Slattery
1	Chief, Vulnerability Br.ESL
1	Chief, C/M Systems Br.ESL
1	Tech Documents Center, ESL
1	Chief, Wire Comm Br.CSL
1	Chief, S&GE Br.CSL
2	Chief, Radio Comm Br.CSL
1	Chief Engineer's Sec. Attn: Mr. Lindner
1	Tech Documents Center, CSL
1	Chief, Power Sources Br.SSL
1	Chief, C&M Br.SSL
1	Chief, Chem Physics Br.SSL
1	Chief, Frequency Control Br.SSL
1	Mr. F. Dickson, Chief, Radio Prop Agency, Bldg 463, Ft Mon
2	AFF Liaison Office, Bldg 611, Ft Mon.
1	Records Holding Area Sec. Watson - File 102B
1	Tech Documents Center, SSL
1	Routing to Dir of Eng, All Sec Chiefs of Eng Div. (Ultimate file SIGEL-DR)
1	OCSigO - SIGEF
1	OCSigO - SIGGD-P1
1	OCSigO - Signal P&O Div. SIGOL-2D
1	Tech Intelligence Library, ERDL, Ft Belvoir, Va.
1	Aberdeen Proving Ground, Md. Attn: Tech Info Unit
1	C/O 9560 TSU, EDL, P.O. Box 205, Mountain View, Calif.
1	Prof. W.G. Dow, Univ. of Michigan, Ann Arbor, Michigan
1	Signal Representative, Officer Group #1, USA Box 65, N.Y.
1	Chief, Plans & Operations Br. - SIGOP-3 - OCSigO
5	ASTIA, Doc Service Center, Knott Bldg, Dayton 2, Ohio

NOTE: Any question re distribution of reports resulting from this contract, or additional copies, please call the Office of Director of Research, Ft. Monmouth, N.J. Eatontown 3-1000 X52135.

SIGEL-DR
12 July 54

Office of Naval Research

Contract N5ori-76

Task Order No. 1

NR-078-011

Technical Report

on

A UHF Impedance Bridge for Shielded Two-Wire Lines

by

Edgar W. Matthews, Jr.

March 10, 1954

The research reported in this document was made possible through support extended Cruft Laboratory, Harvard University, jointly by the Navy Department (Office of Naval Research), the Signal Corps of the U. S. Army, and the U. S. Air Force, under ONR Contract N5ori-76, T. O. 1.

Technical Report No. 184

Cruft Laboratory

Harvard University

Cambridge, Massachusetts

TR 184

A UHF Impedance Bridge for Shielded Two-Wire Lines

by

Edgar W. Matthews, Jr.

Cruft Laboratory, Harvard University

Cambridge, Massachusetts

Abstract

This paper describes an impedance bridge for the ultra-high-frequency range utilizing the shielded two-wire hybrid junction analyzed in Technical Report No. 183. Design and test information are presented for a balance-unbalance detector used to separate the two possible modes, and for an adjustable impedance standard in two-wire line. A description of the equipment used in the experimental work is given, and the results of tests made on the impedance bridge are presented.

- - - - - -

Introduction

Impedance measurement techniques in the UHF range are divided between extensions of low-frequency bridge methods and microwave transmission line procedures; this frequency range seems to be the transition region between the two types of measurement. The accuracy, convenience, and ease of operation afforded by bridges is also possible in the microwave region through the use of hybrid junctions and suitable standards. It is the purpose of this work to develop an impedance bridge for the UHF region utilizing a shielded two-wire hybrid junction as described in Cruft Laboratory Technical Report No. 183. The auxiliary components necessary for use with such a bridge will first be described, and then the experimental equipment employed for testing the bridge. Finally, the results of such tests will be presented.

I

AUXILIARY IMPEDANCE BRIDGE COMPONENTS

A. Balance-Unbalance Detector

Analysis of the shielded two-wire hybrid junction in Technical Report No. 183 has shown that its use as an impedance bridge requires balancing for a null of the balanced mode only at the two detector arms. Consequently, each detector must be designed to respond to a small balanced signal in the presence of a relatively large unbalanced signal. Three possibilities are apparent for the detector:

(1) Attempt to short-circuit the undesired unbalanced signal with an unbalance squelcher (1). This would make the unbalanced detector admittances Y_{CU} and Y_{DU} purely susceptive, and more difficult to match to each other. It seems inherently unwise to introduce deliberately a large reflection from the detectors back into the tee, as it could have serious effects on the accuracy of the bridge.

(2) Utilize a device similar to a coaxial hybrid ring, whereby unbalanced currents are made to cancel by separating the two-wire line into two coaxial lines, inserting a half-wave reversing section in one, and combining in a coaxial tee. This has the disadvantage of frequency sensitivity, requires a difficult initial adjustment for cancellation, and also reflects the unbalanced signal completely.

(3) Design a device similar to Morita and Sheingold's coaxial magic tee (2), which will separate the modes by symmetry alone, and make them both available at separate terminals for proper matching, as desired.

Such a balance-unbalance ("balun") detector has been designed, according to Fig. 1-1, and three models have been built similar to the one shown in Fig. 1-2. Balanced currents excite a voltage across the gap in the direct-coupled shielded loop, and thus are coupled out to the terminal labelled 'balanced output.' Unbalanced currents are coupled out by a direct connection to the center of a bridge across the two-wire line. Quarter-wave sections between elements serve only to eliminate their mutual short-circuiting effect upon each other.

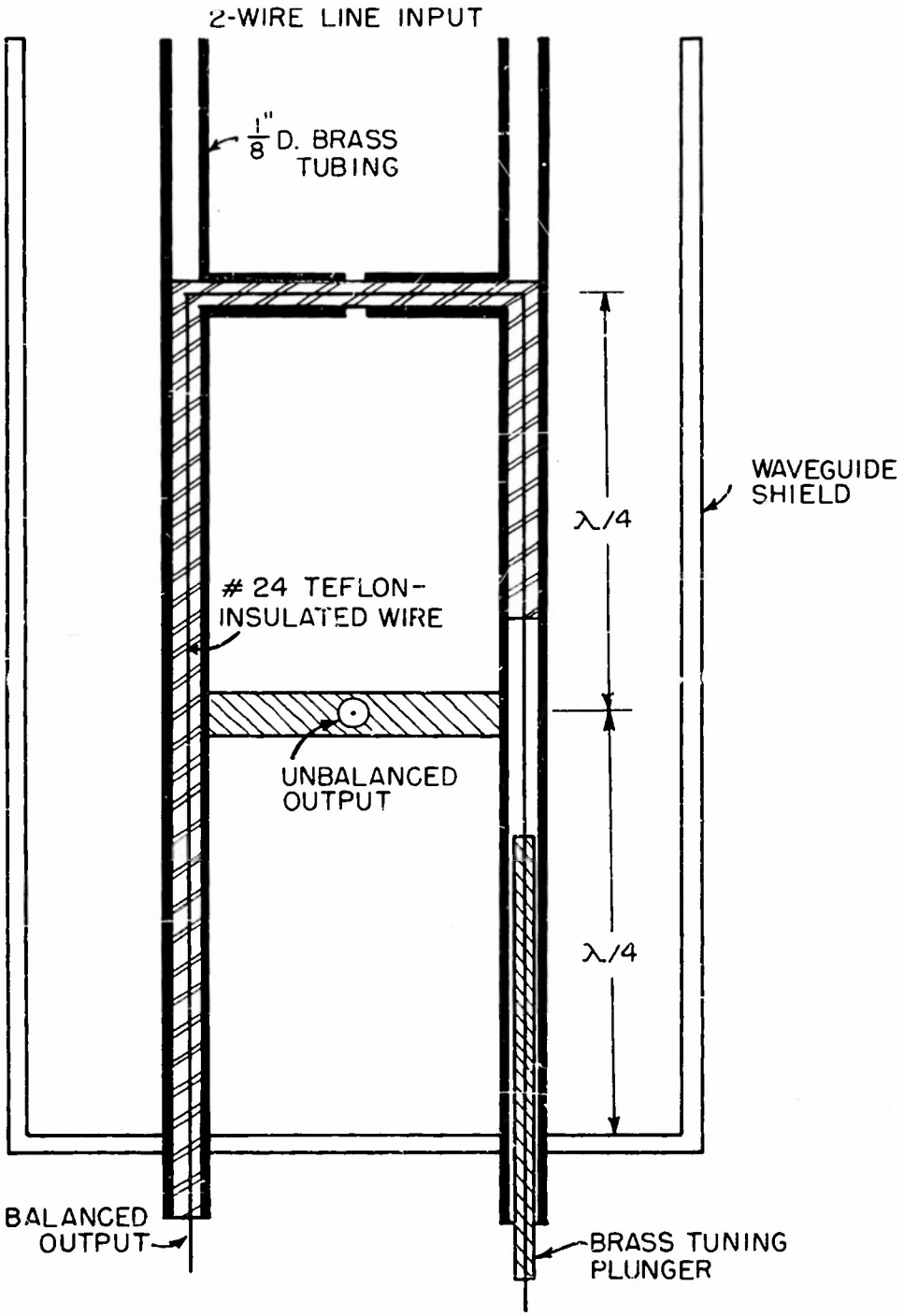

FIG. I - 1 BALANCE - UNBALANCE DETECTOR
(CROSS SECTION)

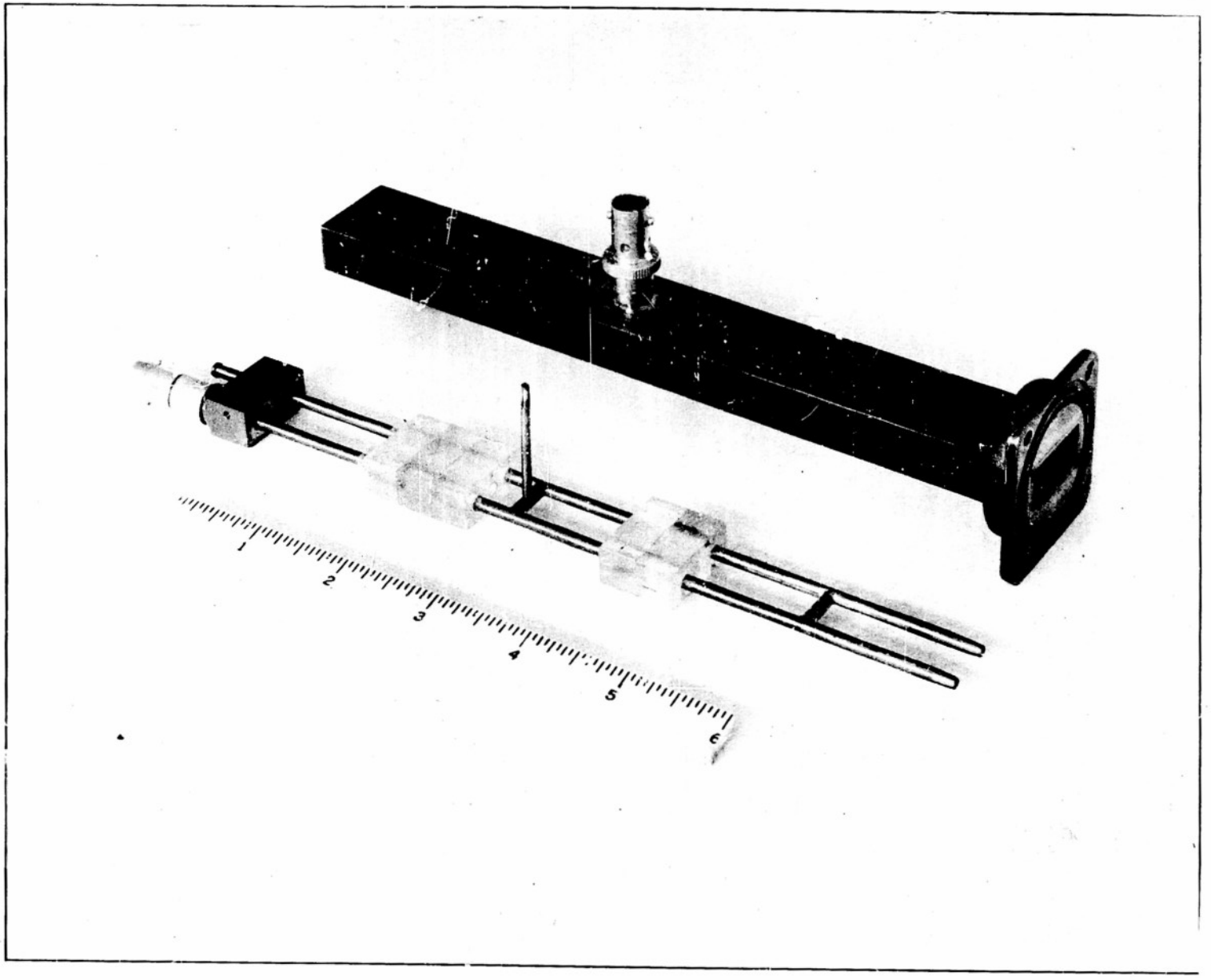

FIG. I–2 BALANCE – UNBALANCE DETECTOR

Separation of the two modes in these balun detectors is thus due entirely to symmetry. Physical construction may allow this separation to be very good, but certainly never perfect. Furthermore, accuracy of the bridge measurements depends very vitally upon this separation, as may be understood from the following development.

The balun detector is essentially a four-terminal-pair network, or a four-port junction, and as such its characteristics can be completely specified by a scattering matrix of the fourth order. Let us define the four terminal-pairs as follows:

Terminals 1 -- Balanced two-wire-line mode
Terminals 2 -- Unbalanced two-wire-line mode
Terminals 3 -- Coaxial terminal coupled mainly to balanced mode
Terminals 4 -- Coaxial terminal coupled mainly to unbalanced mode

If a wave incident on terminal "n" is labelled "a_n", and a wave reflected from terminal "n" is labelled "b_n", the scattering matrix relates these quantities by the matrix equation

$$b = Sa \tag{1-1}$$

By reciprocity, $S_{mn} = S_{nm}$.

Suppose waves are incident on terminals 1 and 2, while terminals 3 and 4 are connected to matched loads ($a_3 = a_4 = 0$); then the output at 3, b_3 (which would normally be adjusted for a null while balancing the bridge for an impedance measurement), is given by

$$b_3 = S_{13} a_1 + S_{23} a_2 \tag{1-2}$$

A null would indicate the condition $S_{13} a_1 = -S_{23} a_2$, which is certainly not the condition for minimum a_1 as desired. Consequently, it is imperative that the ratio S_{23}/S_{13}, or essentially the quantity S_{23}, be as small as possible. Actually, all of the matrix elements which indicate cross-coupling between modes (i.e., S_{23}, S_{14}, S_{12}, and S_{34}) should be small because of the likelihood of some reflection from loads connected to each terminal. Consequently, a measurement of the magnitude of these quantities is necessary to predict the accuracy of impedance bridge measurements.

One of the simplest methods for determining the scattering matrix of a transmission-line junction was originally proposed by Deschamps (3), and modified for practical use by Storer, Stein, and Sheingold (4). This consists of a graphical method using the results of measurements with short-circuit terminations only. The original analysis was developed for a two-terminal-pair network, and later extended by Stein (5) for a multi-terminal junction. This extension, for a four-terminal-pair network, consists of a minimum of 64 independent measurements with short-circuits at various positions on three of the terminal-pairs, together with some formidable mathematical manipulations of the results. Additional accuracy could be secured by making more measurements (preferably 216). Considerable simplification could be achieved if one or more well-matched loads were available. Special difficulties are encountered, however, when applying this method to the balun detectors described above. First, the great difference in magnitude between certain coefficients makes it impossible to measure the small ones by this method -- i.e., no observable change in the input reflection coefficient at terminal 3 occurs for any termination connected to terminal 4. Second, it is difficult to terminate terminals 1 and 2 independently because of their coexistence on the two-wire line. Use can be made of this difference in relative magnitudes, however, to obtain certain of the coefficients by a simple two-terminal-pair Deschamps technique; and the others can be obtained by a special method, as follows.

Case I. Determination of S_{11}, S_{13}, and S_{33}.

Feed power into 3, short-circuit 1 and 2, and match 4.

$$a_3 = 1 \qquad a_4 = 0 \qquad a_1 = -b_1 p^2 \qquad a_2 = -b_2 p^2$$

where $$p = e^{-\gamma \ell} = e^{-j\beta \ell}$$

ℓ = distance from junction reference plane to short-circuit on 1 and 2.

$$b_1 = -S_{11} b_1 p^2 - S_{12} b_2 p^2 + S_{13}$$

$$b_2 = -S_{12} b_1 p^2 - S_{22} b_2 p^2 + S_{23}$$

$$b_3 = -S_{13}b_1p^2 - S_{23}b_2p^2 + S_{33}$$

$$b_4 = -S_{14}b_1p^2 - S_{24}b_2p^2 + S_{34} \qquad (1\text{-}3)$$

$$\therefore \quad b_1 = \frac{S_{13}(1+S_{22}p^2) - S_{12}S_{23}p^2}{(1+S_{11}p^2)(1+S_{22}p^2) - S_{12}^2p^4} \qquad (1\text{-}4a)$$

$$b_2 = \frac{S_{23}(1+S_{11}p^2) - S_{12}S_{13}p^2}{(1+S_{11}p^2)(1+S_{22}p^2) - S_{12}^2p^4} \qquad (1\text{-}4b)$$

$$b_3 = S_{33} - p^2\,\frac{S_{13}^2(1+S_{22}p^2) + S_{23}^2(1+S_{11}p^2) - 2S_{12}S_{13}S_{23}p^2}{(1+S_{11}p^2)(1+S_{22}p^2) - S_{12}^2p^4} \qquad (1\text{-}5)$$

Now if $S_{12}^2 \ll 1$ and $S_{23}^2 \ll S_{13}^2$, this reduces to

$$b_3 = S_{33} - \frac{S_{13}^2p^2}{1 + S_{11}p^2} \qquad (1\text{-}5a)$$

This is the same type of equation as characterizes a two-terminal-pair network, for which a simple Deschamps' measurement of the input reflection coefficient $\Gamma_3 = b_3/a_3$ for two or more pairs of values of p, each pair separated by $\lambda/4$, will permit determination of S_{11}, S_{13}, and S_{33}. The inequalities specified for the simplification of b_3 in (1-5) above are easily satisfied for the balun detectors under measurement, as will be seen from the results. The specification of a match on terminal 4 is very lax because of the relative magnitudes of S_{34} and S_{14}.

Case II. Determination of S_{22}, S_{24}, and S_{44}.

Feed power into 4, short-circuit 1 and 2, and match 3. This case is exactly analagous to Case I, with the result:

$$b_4 = S_{44} - p^2\,\frac{S_{14}^2(1+S_{22}p^2) + S_{24}^2(1+S_{11}p^2) - 2S_{12}S_{14}S_{24}p^2}{(1 + S_{11}p^2)(1 + S_{22}p^2) - S_{12}^2p^4} \qquad (1\text{-}6)$$

and if $S_{12}^2 \ll 1$ and $S_{14}^2 \ll S_{24}^2$, this reduces to

$$b_4 = S_{44} - \frac{S_{24}^2 p^2}{1 + S_{22} p^2} \tag{1-6a}$$

from which S_{22}, S_{24}, and S_{44} can be determined by a Deschamps' measurement.

No further information of interest is available with a short-circuit on both terminals 1 and 2 simultaneously. It is fairly easy, however, to build a device which will short-circuit the balanced mode on the two-wire line (terminals 1) with a wire bridge across the line, while providing a tap at the center of this bridge for connection to the unbalanced mode (terminals 2). If this device is to be used to measure the separation of modes in the balun detectors, it will have to be constructed very precisely so that it does not couple the modes itself. Such a device has been built, as shown in Fig. 1-3, which provides a sliding short circuit for the balanced mode with a fine screw adjustment for accurate positioning. With this, it is possible to make the measurements described in Cases III and IV. It is assumed that only the magnitude of the small junction scattering coefficients is desired.

Case III. Determination of S_{12} and S_{23}.

Feed power into 2, short-circuit 1, and match 3 and 4.

$$a_2 = 1 \qquad a_1 = -b_1 p^2 \qquad a_3 = a_4 = 0 \qquad p = e^{-j\beta\ell}$$

$$b_1 = -b_1 p^2 S_{11} + S_{12} \qquad b_3 = -b_1 p^2 S_{13} + S_{23} \tag{1-7}$$

$$b_2 = -b_1 p^2 S_{12} + S_{22} \qquad b_4 = -b_1 p^2 S_{14} + S_{24}$$

from which, immediately, $b_1 = S_{12}/(1 + S_{11} p^2)$, so

$$\frac{b_3}{b_4} = \frac{S_{23} - b_1 p^2 S_{13}}{S_{24} - b_1 p^2 S_{14}} = \frac{S_{23}(1 + S_{11} p^2) - p^2 S_{12} S_{13}}{S_{24}(1 + S_{11} p^2) - p^2 S_{12} S_{14}} \tag{1-8}$$

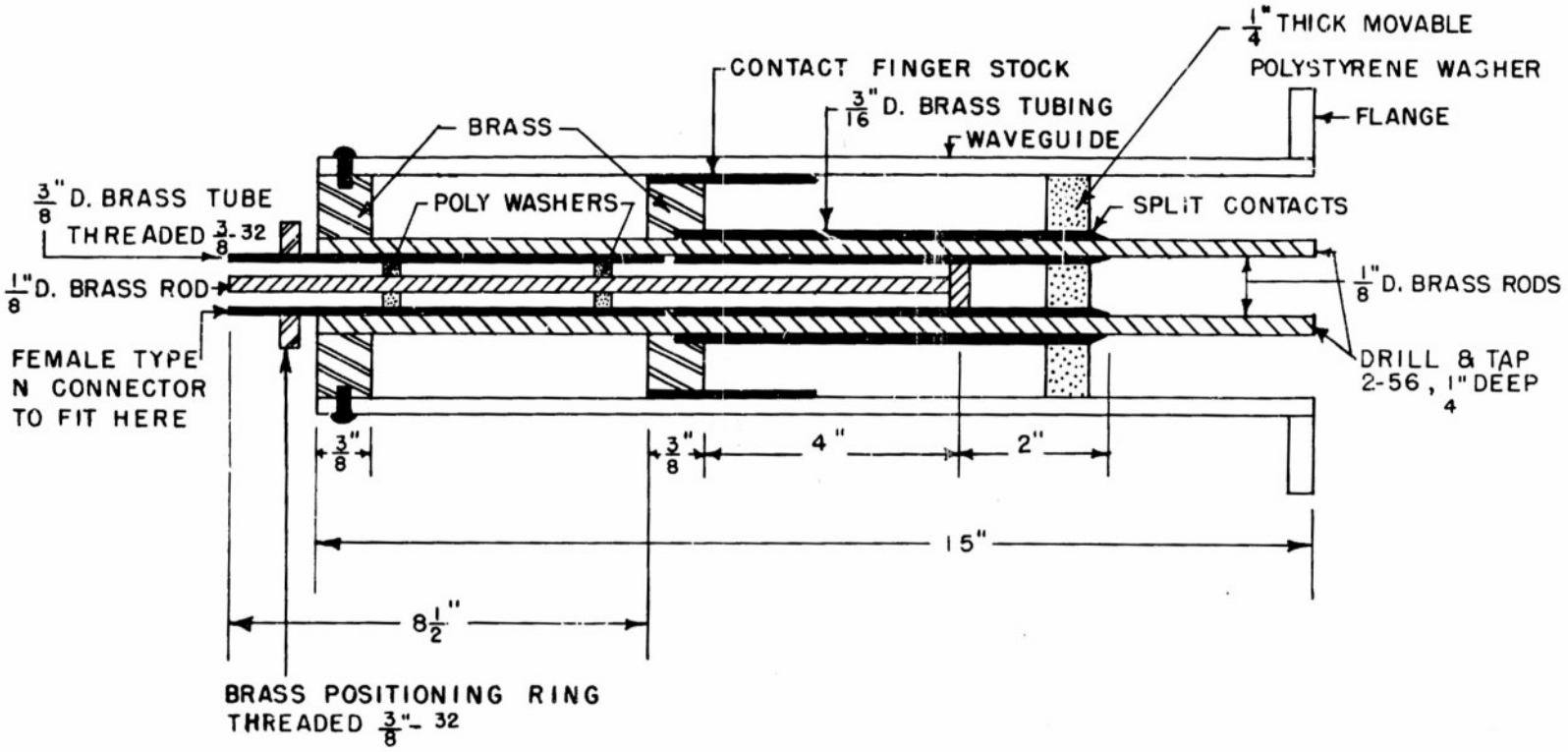

FIG. 1-3 SLIDING BALANCE SHORTING SECTION

and assuming the inequality $S_{12}S_{14} \ll 1$, this becomes

$$\frac{b_3}{b_4} = \frac{S_{23}}{S_{24}} - \frac{p^2 S_{12}S_{13}}{S_{24}(1+S_{11}p^2)} = \frac{S_{23}}{S_{24}}\left[\frac{1 + p^2(S_{11} - \frac{S_{12}S_{13}}{S_{23}}}{1 + S_{11}p^2}\right] = \frac{S_{23}}{S_{24}}\left[\frac{1+S_{123}p^2}{1+S_{11}p^2}\right] \quad (1-8a)$$

where

$$S_{123} = S_{11} - \frac{S_{12}S_{13}}{S_{23}}$$

Now call $2\beta\ell = \frac{4\pi\ell}{\lambda} = \theta$, $S_{123} = a\, e^{j\alpha}$,

$$S_{11} = b\, e^{j\beta} \ , \quad K = \left|\frac{S_{23}}{S_{24}}\right|^2 \ , \quad \text{and} \quad x = \left|\frac{b_3}{b_4}\right|^2 \ .$$

Combining these definitions with (1-8a),

$$x = K\left|\frac{1+ae^{j(\alpha-\theta)}}{1+be^{j(\beta-\theta)}}\right|^2 = K\left|\frac{1+a[\cos(\alpha-\theta)+j\sin(\alpha-\theta)]}{1+b[\cos(\beta-\theta)+j\sin(\beta-\theta)]}\right|^2$$

$$= K\,\frac{[1+a\cos(\alpha-\theta)]^2+a^2\sin^2(\alpha-\theta)}{[1+b\cos(\beta-\theta)]^2+b^2\sin^2(\beta-\theta)} = K\left[\frac{1+a^2+2a\cos(\alpha-\theta)}{1+b^2+2b\cos(\beta-\theta)}\right] \quad (1-9)$$

Let four measurements be taken of the quantity x for positions of the short circuit corresponding to the following values of θ:

$$\theta_1 = \theta_o \qquad \theta_2 = \theta_o + \frac{\pi}{2} \qquad \theta_3 = \theta_o + \pi \qquad \theta_4 = \theta_o + \frac{3\pi}{2}$$

$$x_1 = K\left[\frac{1+a^2+2a\cos(\alpha-\theta_o)}{1+b^2+2b\cos(\beta-\theta_o)}\right] \qquad x_2 = K\left[\frac{1+a^2+2a\sin(\alpha-\theta_o)}{1+b^2+2b\sin(\beta-\theta_o)}\right] \quad (1-10)$$

$$x_3 = K\left[\frac{1+a^2-2a\cos(\alpha-\theta_o)}{1+b^2-2b\cos(\beta-\theta_o)}\right] \qquad x_4 = K\left[\frac{1+a^2-2a\sin(\alpha-\theta_o)}{1+b^2-2b\sin(\beta-\theta_o)}\right]$$

If the following definitions are made,

$$A = 1 + b^2 + 2b\cos(\beta-\theta_o) \qquad B = 1 + b^2 + 2b\sin(\beta-\theta_o)$$

$$C = 1 + b^2 - 2b\cos(\beta-\theta_o) \qquad D = 1 + b^2 - 2b\sin(\beta-\theta_o)$$

then (1-10) can be written as:

$$x_1A = K[1 + a^2 + 2a\cos(\alpha-\theta_o)] \qquad x_2B = K[1 + a^2 + 2a\sin(\alpha-\theta_o)]$$

$$x_3C = K[1 + a^2 - 2a\cos(\alpha-\theta_o)] \qquad x_4D = K[1 + a^2 - 2a\sin(\alpha-\theta_o)] \tag{1-11}$$

and thus, by inspection, the following relations hold:

$$x_1A + x_3C = x_2B + x_4D = 2K(1+a^2) \equiv n \tag{1-12}$$

$$x_1A - x_3C = 4aK\cos(\alpha-\theta_o)$$

$$x_2B - x_4D = 4aK\sin(\alpha-\theta_o)$$

$$(x_1A - x_3C)^2 + (x_2B - x_4D)^2 = 16a^2K^2 \equiv 16u \tag{1-13}$$

Solving (1-12) and (1-13) for K,

$$2K^3 - nK^2 + 2uK = 0 \tag{1-14}$$

which has solutions, other than the trivial one K = 0,

$$K = \frac{n \pm \sqrt{n^2 - 16u}}{4} \quad ; \quad \text{then} \quad a = \frac{\sqrt{u}}{K}$$

$$\alpha = \cos^{-1}\left[\frac{1}{2a}\left(\frac{x_1A}{K} - 1 - a^2\right)\right] + \theta_o \tag{1-15}$$

If S_{11}, S_{13}, and S_{24} are known from Cases I and II, then

$$|S_{23}|^2 = K|S_{24}|^2 \tag{1-16a}$$

and by definition,

$$\frac{S_{12}S_{13}}{S_{23}} = S_{11} - S_{123} = b e^{j\beta} - a e^{j\alpha}$$

$$\left|S_{12}\right| = \left|\frac{S_{23}}{S_{13}}\right| \left|b e^{j\beta} - a e^{j\alpha}\right| \qquad (1\text{-}16b)$$

Case IV. Determination of S_{14} and S_{34}.

Feed power into 4, short-circuit 1, and match 2 and 3. This case is exactly analagous to Case III, with the results:

$$\frac{b_3}{b_2} = \frac{S_{34}}{S_{24}}\left[\frac{1 + p^2(S_{11} - \frac{S_{13}S_{14}}{S_{34}})}{1 + S_{11}p^2}\right] = \frac{S_{34}}{S_{24}}\left[\frac{1 + S_{134}p^2}{1 + S_{11}p^2}\right] \qquad (1\text{-}17)$$

where

$$S_{134} = S_{11} - \frac{S_{13}S_{14}}{S_{34}}$$

Define:

$$S_{134} = c e^{j\gamma} \quad , \quad M = \left|\frac{S_{34}}{S_{24}}\right|^2 \quad , \quad \text{and} \quad y = \left|\frac{b_3}{b_2}\right|^2$$

and if θ, S_{11}, A, B, C, and D are defined as before, then

$$y_1A + y_3C = y_2B + y_4D = 2M(1+c^2) \equiv h$$

$$y_1A - y_3C = 4cM\cos(\gamma - \theta_o)$$

$$y_2B - y_4D = 4cM\sin(\gamma - \theta_o) \qquad (1\text{-}18a)$$

$$(y_1A - y_3C)^2 + (y_2B - y_4D)^2 = 16\,c^2M^2 \equiv 16d \qquad (1\text{-}18b)$$

Solving these as before,

$$M = \frac{h \pm \sqrt{h^2 - 16d}}{4} \qquad c = \frac{\sqrt{d}}{M} \qquad (1\text{-}19)$$

$$\gamma = \cos^{-1}\left[\frac{1}{2c}\left(\frac{y_1 A}{M} - 1 - c^2\right)\right] + \theta_o$$

$$|S_{34}|^2 = M|S_{24}|^2 \quad \text{and} \quad |S_{14}| = \left|\frac{S_{34}}{S_{13}}\right| |be^{j\beta} - ce^{j\gamma}| \qquad (1\text{-}20)$$

Experimental Procedure

Cases I and II. Measurements of input reflection coefficients were made on the coaxial slotted line described in Chapter II; the connection between slotted line and balun detector was made as smooth as possible with a tapered section from the 7/8-inch line to a Type N connector, and a Type N to BNC adapter specially constructed for low reflections. The short circuit was provided by the device shown in Fig. 1-3. Measurements of the magnitude of the reflection coefficients were not taken, as the balun detector was assumed lossless; actually, the VSWR's observed were at least 30, and approached 100 when a short-circuiting plate was used to terminate the two-wire terminals to establish a reference plane, indicating that the losses present were mostly in the short-circuiting device. Since the screw adjustment on this device has a 3/8-32 thread, the wavelength was adjusted to 16 inches, or 40.6405 cm, so that $\lambda/16$ = 1 inch = 32 threads. Data were taken for four pairs of points, or eight positions of the short circuit, spaced $\lambda/16$ apart; this provided a good check on the experimental results. Graphical plots were made of the data, according to Deschamps' method, and the results are given in the next section (Table 1-1). Consistency of the data indicates an accuracy of 0.5% or better.

Cases III and IV. In order to determine the magnitude of the ratio b_3/b_4, matched crystal detectors were connected to both terminals 3 and 4, the input was adjusted to hold the output at 4 constant, and the relative output at 3 was observed on the calibrated detector-amplifier combination, as the position of the short circuit on terminal 1 was varied. The absolute magnitude of the ratio was then determined by connecting the terminal-3 detector on terminal 4 through an appropriate amount of calibrated lossy cable. The detectors were matched by means

of the coaxial slotted line. The same procedure was used for obtaining the ratio b_3/b_2, except that the detector on terminal 2 was matched through the short-circuiting device by means of the two-wire slotted line.

Data were again taken for eight positions of the short circuit; since four points are sufficient to determine the desired quantities, a check on the experimental data was provided. This was found very necessary, as the results depend critically on proper matching at the terminals to which the detectors were connected, which may be difficult to achieve, especially at terminal 2 over the entire range of the short-circuiting device. Several sets of data were taken, and only those which exhibited internal consistency were used. This consistency was established by computing the angle $\phi_o = \beta - \theta_o$ which would be necessary for each set of four points to fit an equation of the type given in (1-10), and comparing this with the independently determined values of β and θ_o. The formula for ϕ_o can be derived from (1-10) by elimination of K, a, and $(a-\theta_o)$ to give

$$\sin(\phi_o+\phi) = \frac{1+b^2}{2b}\left[\frac{x_1-x_2+x_3-x_4}{\sqrt{(x_1-x_3)^2+(x_2-x_4)^2}}\right], \quad \tan\phi = \frac{x_3-x_1}{x_2-x_4} \qquad (1\text{-}21)$$

Results of the measurements are given in Table 1-1. It will be noted that two sets of results are obtained for each detector, because of the quadratic form of Eqs. (1-14) and (1-19). These are not greatly different, and are thus useful for determining the maximum possible value of each quantity. This duplicity can be resolved only by a different type of measurement, involving relative phase.

The quantity most directly involved in the accuracy of bridge measurements is, from Eq. (1-2), S_{23}. Values for both detectors indicate a separation of modes on this basis of $20 \log_{10}(.012) = -38.4$ db.

Table 1-1

Measured Balun Detector Coefficients

Cases I and II.

	Detector No. 1	Detector No. 2
S_{11}	$.327 \angle 61.2^\circ$	$.343 \angle 55.8^\circ$
S_{13}	$.945 \angle -132.2^\circ$	$.939 \angle -133.6^\circ$
S_{33}	$.327 \angle -145.5^\circ$	$.343 \angle -143.0^\circ$
S_{22}	$.458 \angle 110.4^\circ$	$.502 \angle 113.6^\circ$
S_{24}	$.889 \angle -51.4^\circ$	$.865 \angle -25.1^\circ$
S_{44}	$.458 \angle 18.2^\circ$	$.502 \angle 16.4^\circ$

Cases III and IV.

$\lvert S_{12} \rvert$	.0103,	.0143	.0138,	.0140
$\lvert S_{23} \rvert$	.0117,	.00631	.0122,	.0118
$\lvert S_{14} \rvert$	.00756,	.00780	.00598,	.00898
$\lvert S_{34} \rvert$	.00587,	.00553	.00698,	.00328

B. Adjustable Standard Impedance

An impedance bridge utilizing the two-wire hybrid junction previously described is inherently a null-measuring device, and requires for its operation an adjustable calibrated standard impedance. When the standard impedance is made equal to the unknown impedance under measurement, the bridge output is reduced to zero, and a condition of "bridge balance" is said to exist. The value of the unknown is then determined from the settings of the standard impedance. With this bridge, there is no simple way of applying a multiplicative factor to the standard for comparison with the unknown, as with the "ratio arms" of a Wheatstone bridge; consequently, the range of adjustment of the standard is exactly the range of measurement of the bridge. The problem of obtaining such a standard is further enhanced by the coexistence of two modes of propagation on the shielded two-wire line. For the present, however, attention will be centered only on the balanced mode. Structures used for both standard and unknown

impedances will be kept as nearly symmetrical as possible, to reduce coupling between modes; and everything possible will be done to suppress or balance out the unbalanced mode.

1. Design of the Standard Impedance

Since there are no commonly available adjustable attenuators and phase shifters for two-wire line, it seems logical to consider a device using adjustable stubs for the standard impedance. A stub is considered to be a lossless short-circuited length of line connected in shunt across a transmission line. Its normalized input admittance is

$$y_{in} = \frac{Y_{in}}{Y_c} = -j \cot \beta \ell$$

Consider a pair of stubs separated by a distance w connected to a line terminated by a fixed admittance y_s, as shown in Fig. 1-4. (All admittances are normalized in terms of the characteristic admittance of the line.) The input admittance to the combination is given, according to standard transmission-line formulas, by

$$y_{in} = \frac{(y_s + jb_1) + j \tan \beta w}{1 + j(y_s + jb_1) \tan \beta w} + jb_2 = g_{in} + jb_{in} \quad . \tag{1-22}$$

When separated into real and imaginary parts, this becomes

$$g_{in} = \frac{g_s \sec^2 \beta w}{[g_s^2 + (b_s + b_1)^2] \tan^2 \beta w - 2(b_s + b_1) \tan \beta w + 1} \tag{1-22a}$$

$$b_{in} = \frac{(b_s + b_1 + \tan \beta w)[1 - (b_s + b_1) \tan \beta w] - g_s^2 \tan \beta w}{[g_s^2 + (b_s + b_1)^2] \tan^2 \beta w - 2(b_s + b_1) \tan \beta w + 1} + b_2 \tag{1-22b}$$

Because of the additive b_2 term in (1-22b), any desired value of b_{in} may be obtained, so the only limit of adjustment is on g_{in}. This can easily be interpreted on a Smith chart, where the locus of admittances at the first stub, represented by $y_s + jb_1$, is the circle $g = g_s$. A transformation to the second stub rotates this locus by an amount βw, and the maximum

g_{in} occurs where this rotated locus becomes tangent to another constant g circle. In the limit as $w \longrightarrow \lambda/2$, $g_{max} \longrightarrow \infty$; this, however, requires very fine adjustment of the first stub, so that accuracy is sacrificed for range. In practice, a compromise must be made between the two, and this is frequently chosen as $w = 3\lambda/8$. For this case,

$$g_{in} = \frac{2g_s}{g_s^2 + (1+b_s+b_1)^2} \leq \frac{2}{g_s} \quad , \quad w = \frac{3\lambda}{8} \tag{1-23}$$

Another compromise between range and accuracy must be made in choosing g_s. Obviously, no combination of values of w and g_s will permit accurate measurement of the complete range of conductance from zero to infinity, so that a third factor must be introduced. One possibility is insertion of a quarter-wave section of line in either the standard or the unknown arm of the bridge, with which $g_{in} \geq g_s/2$. Large values of g_{in} can thus be measured with the quarter-wave section, small values without the section, and the middle range $g_s/2 \leq g_{in} \leq 2/g_s$ with either. A reasonable-sized middle range is desirable in order to minimize changing the quarter-wave section without sacrificing accuracy; this would be provided by $g_s = 1$.

If insertion of a quarter-wave section is inconvenient, the third variable may be chosen to be a third stub, appropriately placed with respect to the first two. Its movement may be restricted to a number of fixed positions, in order to simplify calibration. Another possibility is to provide a switching arrangement for selection of y_s from a number of fixed values; however, it is apparent from the above discussion that range can be extended in this manner only at the expense of accuracy. Alternatively, range can be reduced by this means if particular accuracy is desired within the reduced range.

Many other schemes for obtaining an adjustable standard impedance present themselves, such as the use of sliding sections or movable stubs, with helical springs for line conductors to avoid the sliding contact problem. Some are not feasible from a mechanical or electrical stability standpoint; others require an excessive amount of development work, which is not the object of this research. Most would require some sort

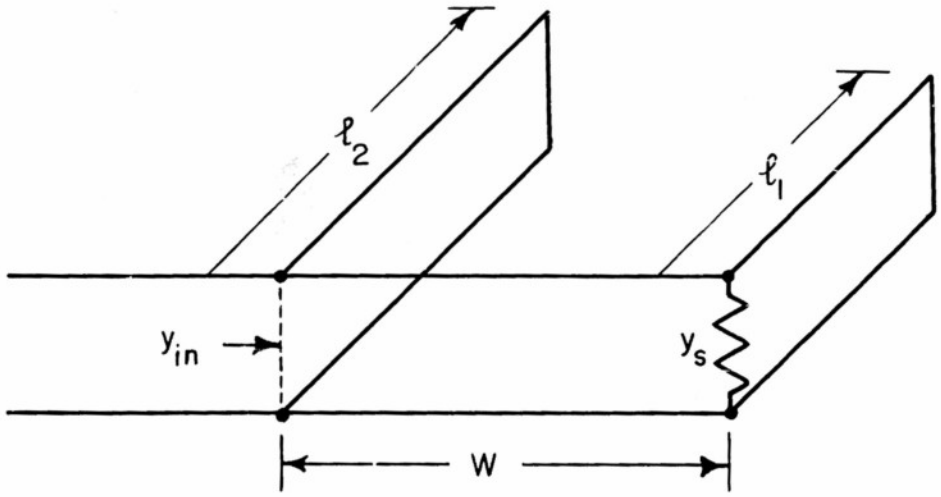

FIG. I-4 ADJUSTABLE LOAD SCHEMATIC DIAGRAM

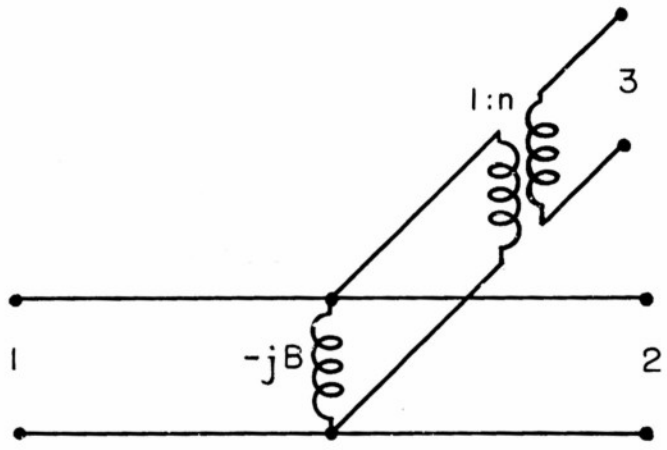

FIG. I-5 SHUNT TEE EQUIVALENT CIRCUIT

of point-by-point calibration, while the combination analyzed above requires only experimental confirmation that the elements involved behave according to their idealized transmission-line equivalents. Consequently, attention was centered experimentally on the double-fixed-stub scheme, with optional quarter-wave section; and an analysis of the characteristics of the individual elements follows.

2. Shielded Two-Wire Tee-Junction

For purposes of calibration of the standard adjustable load, it is desired to examine the characteristics of a shielded two-wire tee-junction, which is to be used as a shunt stub. At low frequencies, a tee-junction appears to be a simple shunt circuit, for which the voltage at the junction point is common to all three lines, and the currents entering the junction from the three lines must add vectorially to zero. The concept of characteristic impedance of each of the three lines is unimportant, as the lengths of line usually involved are small fractions of a wavelength. As the frequency is raised, however, terminal effects arise in the vicinity of the junction, just as in the case of a dipole antenna center-fed from a two-wire line (6). Line parameters (inductance and capacitance per unit length) are not constant, because of the discontinuity of current and the capacitive coupling among all three lines near the junction. Furthermore, differences in characteristic impedance of the three lines produce different effective couplings to the junction. Additional difficulties may be encountered in the case of the shielded two-wire tee, because of the effect of images caused by the shield. If the frequency is not too high, so that distributed coupling effects may be accounted for by a lumped equivalent circuit located at the junction, the symmetry of the tee should allow use of the equivalent circuit for a coaxial tee as given by Harrison (7), and shown in Fig. 1-5.

This circuit is valid only between certain reference planes in each arm, whose location thus actually forms part of the equivalent circuit. The reference planes are established by utilizing the low-frequency performance of the equivalent circuit, i.e., when a short circuit is placed on one of the arms, it should appear also at the terminals of the other two arms, and no transmission of power should take place between the other two arms.

Experimentally, a short circuit is placed on arm 3 (the stub arm) and adjusted in position until there is a minimum of power transmitted between arms 1 and 2. (This power does not reduce to zero because of finite losses in the stub arm.) The location of the short circuit on arm 3 is then the location of the reference plane for arm 3, and the positions of the voltage minima on arms 1 and 2 (as each, in turn, is fed) are the reference planes for these arms.

The determination of the quantities n (the ideal transformer turns ratio) and B (the shunt susceptance) of the equivalent circuit in Fig. 1-5 is easily accomplished by taking a series of measurements of the input admittance at arm 1 as a function of positions of short circuits on both arms 2 and 3. If the actual susceptances presented at the reference planes 2 and 3 for particular positions j and k of the short circuits on 2 and 3, respectively, are represented by B_2^j and B_3^k, then the total input susceptance B_1^{jk} at reference plane 1 will be

$$B_1^{jk} = B + B_2^j + n^2 B_3^k \tag{1-24}$$

For another position m of the short circuit on 3,

$$B_1^{jm} = B + B_2^j + n^2 B_3^m \tag{1-24a}$$

$$\therefore n^2 = \frac{B_1^{jk} - B_1^{jm}}{B_3^k - B_3^m} = \frac{\sum_k (-1)^k B_1^{jk}}{\sum_k (-1)^k B_3^k} \tag{1-25}$$

B_2 and B_3 are computed from the relation for a lossless short-circuited line, $B = -\cot \beta \ell$. The latter form of (1-25) is convenient if more than two measurements are taken for increased accuracy; the total number of measurements must be even. Once n^2 has been determined, B can be found as

$$B = B_1^{jk} - B_2^j - n^2 B_3^k = -B_2^j + \frac{1}{N} \sum_{k=1}^{N} (B_1^{jk} - n^2 B_3^k) \tag{1-26}$$

with an average being taken for all values of k as indicated. Additional

accuracy for both n^2 and B can be obtained by repeating the measurements for additional values of j; i.e., positions of the short circuit on arm 2.

Measurements were made on two different stubs, for use in the double-stub adjustable standard impedance. Results of the stub measurements are as follows:

	n^2	B	Distance from Flange to Ref. Planes 1 and 2	Shunt Arm Scale Reference Position
Stub 1	1.016	-.057	5.039 cm	17.97 cm
Stub 2	1.009	-.024	5.038 cm	23.005 cm

For values of B_1 and B_3 less than 3, the data checked within 0.5%; the value of B, however, is not so accurate because it is calculated as the difference between two larger quantities. It is interesting to note that the values of n^2 are comparable to $\sqrt{\epsilon}$ for polyfoam (1.012 to 1.016), which was used in the stubs for supporting the center conductors. Thus it would seem that a first approximation to the value for n^2 of a tee with two symmetrical arms would be the ratio of the characteristic impedances of the stub arm and the two symmetrical arms.

3. Load Calibration

The adjustable standard impedance desired consists of two shunt stubs separated by $3\lambda/8$, terminated by a fixed resistance unit, preferably fairly well matched to the line. Since it is further desired to suppress the unbalanced mode as much as possible, and to avoid coupling to it by any asymmetries, it was decided to build the fixed resistance unit from a single carbon resistor (1/4-watt) connected symmetrically between the line wires. After considerable experimentation, a 68-ohm resistor was used, connected to a length of line supported by a 1 3/4-inch block of solid polystyrene; a very well-matched load resulted from this combination. It was screwed directly onto stub 1 to avoid friction contacts, and the entire unit calibrated on the slotted line as a function of stub position with the result that the fixed load was found to have a value $y_s = 1.0013 + j.0476$, including the shunt susceptance B of the equivalent stub circuit.

The actual value of the adjustable standard impedance at the reference plane of the input stub may now be calculated as a function of the two stub positions. The input conductance depends only on the first stub, while the

susceptance is the sum of the two components, b'_1 and b'_2, each a function of only one stub; consequently, single-parameter calibration tables will suffice, but two components will have to be added to obtain the susceptance. Substitution of the above value of y_s into Eq. (1-22) gives

$$y_{in} = \frac{1.0013 + j(.0476 - n_1^2 \cot \beta\ell_1) + j \tan \beta w}{1 + j \tan \beta w [\, 1.0013 + j(.0476 - n_1^2 \cot \beta\, \ell_1)]} - j\, n_2^2 \cot\, \beta\ell_2 + jB_2 \quad (1\text{-}27)$$

where $B_2 = -.024$, $n_1^2 = 1.016$, $n_2^2 = 1.009$, and the quantities $\beta\ell_1$ and $\beta\ell_2$ are the distances from the stub scale reference positions to the actual stub positions. The value of w is the sum of the distances from the two stub input flanges to their reference planes, plus the actual distance between stub flanges; this becomes

$$w = 5.038 + 5.039 + 4.661 = 14.738 \text{ cm}$$

At 738.2 mc, $\beta w = 130.55^\circ$ and $\tan \beta w = -1.1688$, and Eq. (1-27) becomes

$$y_{in} = \frac{1.0013 - j[\, 1.1212 + n_1^2 \cot \beta\ell_1]}{1.0556 - 1.1688\, n_1^2 \cot\beta\, \ell_1 - j\, 1.1703} - jn_2^2 \cot \beta\ell_2 + jB_2 \quad (1\text{-}28)$$

This can be separated into real and imaginary parts, and the latter further separated into contributions from each of the two stubs, as follows:

$$y_{in} = g_{in} + jb_{in} = g_1 + jb'_1 + jb'_2 \quad (1\text{-}29)$$

$$g_1 = \frac{2.3691}{(1.0556 - 1.1688\, n_1^2 \cot\, \beta\ell_1)^2 + 1.3696} \quad (1\text{-}30a)$$

$$b'_1 = \frac{1.1718 - (1.1212 + n_1^2 \cot \beta\ell_1)(1.0556 - 1.1688\, n_1^2 \cot\, \beta\ell_1)}{(1.0556 - 1.1688\, n_1^2 \cot\, \beta\ell_1)^2 + 1.3696} \quad (1\text{-}30b)$$

$$b'_2 = -\, n_2^2 \cot\, \beta\ell_2 + B_2 \quad (1\text{-}30c)$$

These functions are tabulated in Table 1-2.

The input impedance with the quarter-wave section in front of the standard impedance is the same as the above admittance. The input

Table 1-2. Standard Load Calibration

Stub 1 Pos.	g_1	b'_1	Stub 1 Pos.	g_1	b'_1
3	1.7280	.9102	17	.02925	.6326
4	1.6472	.4866	18	.000037	.8622
5	1.4584	.2265	18.5	.01302	1.0051
6	1.2602	.08633	19	.05692	1.1642
7	1.0816	.01826	19.5	.14481	1.3347
8	.9261	-.00715	20	.29092	1.5027
9	.7900	-.00607	20.5	.5048	1.6420
10	.6689	.01319	21	.7811	1.7171
11	.5588	.04666	21.5	1.0868	1.6915
12	.4566	.09314	22	1.3727	1.5557
13	.3598	.15353	22.5	1.5856	1.3338
14	.2667	.23091	23	1.7018	1.0736
15	.17789	.33017	24	1.6922	.6036
16	.09579	.4599	25	1.5229	.29434
17	.02925	.6326	26	1.3222	.12130

Table 1-2 Cont'd. Standard Load Calibration

Stub 2 Pos.	b'_2	Stub 2 Pos.	b'_2
8	-.9619	21.5	4.2325
9	-.7061	22	6.418
10	-.4986	22.5	12.89
11	-.3195	23	1156
12	-.1564	23.5	-13.185
13	.0002	24	-6.528
14	.1582	24.5	-4.3137
15	.3251	25	-3.1912
16	.5114	25.5	-2.5083
17	.7312	26	-2.0443
18	1.0086	26.5	-1.7051
19	1.3912	27	-1.4443
19.5	1.6517	28	-1.0594
20	1.9892	29	- .7813
20.5	2.4502	30	- .5611
21	3.1245	31	- .3749
21.5	4.2325	32	- .2075

admittance with, or the input impedance without, the quarter-wave section is just the reciprocal of the above value; these reciprocals, however, cannot be tabulated easily because they are not simple additive functions of the two stub positions.

Because of the large scale necessary to plot the above relations, in order to cover the full range of values, it is felt that more accuracy can be obtained by quadratic interpolation between the calculated values given in Table 1-2. This was actually done for the evaluation of measurements in Chapter III. For general use, the process of interpolation can be facilitated by an auxiliary table of differences related to the first and second derivatives at each calculated stub position.

II

MEASURING EQUIPMENT

The experimental setup for impedance measurements using the two-wire hybrid junction shown in Fig. 2-1 is outlined on the block diagram of Fig. 2-2 and illustrated in Fig. 2-3. It begins with a 750-megacycle transmitter, square-wave modulated at 1000 cycles, filtered and monitored, feeding the hybrid junction through a balun, such as described in Chapter I. The standard load and the impedance under measurement (which may consist of an antenna over a ground screen which terminates the waveguide shield) are connected to symmetrical arms of the bridge, and the error signal is extracted from the other two symmetrical arms through balun detectors, to eliminate the undesired unbalanced mode. This signal is detected by a 1N21B crystal, amplified, and read on a Ballantine a-c voltmeter.

Calibration measurements were made on a two-wire slotted line, using the same transmitting and detecting equipment, as illustrated in Fig. 2-4. A coaxial slotted line was used for measurement of the balun detector characteristics.

Constructional and operational details of the individual components of the measuring system follow.

A. Transmitter

The 750-megacycle source used for all of the measurements was a modified APT-6 transmitter utilizing a 3C22 lighthouse tube in a double coaxial cavity. Its circuit is shown, together with modulator and power supply, in Fig. 2-5.

In order to obtain satisfactory stability, it was found necessary to use a line-voltage stabilizer for all of the measuring equipment; and in addition, a regulated power supply was designed and built for the transmitter. This consists of a conventional degenerative-amplifier regulator capable of supplying 100 milliamperes at 900 or 1200 volts (selected by a switch on the front panel).

Modulation is accomplished by introducing a 1000-cycle square wave into the cathode circuit of the oscillator tube to switch it on and off. The

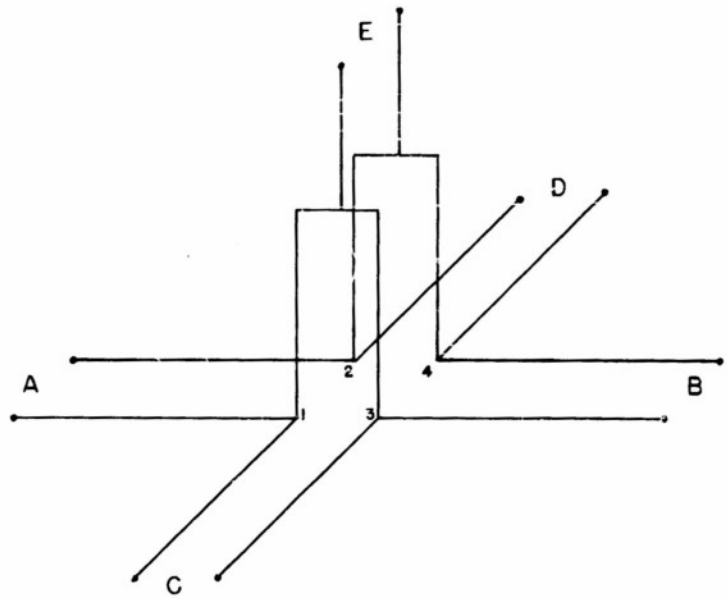

a

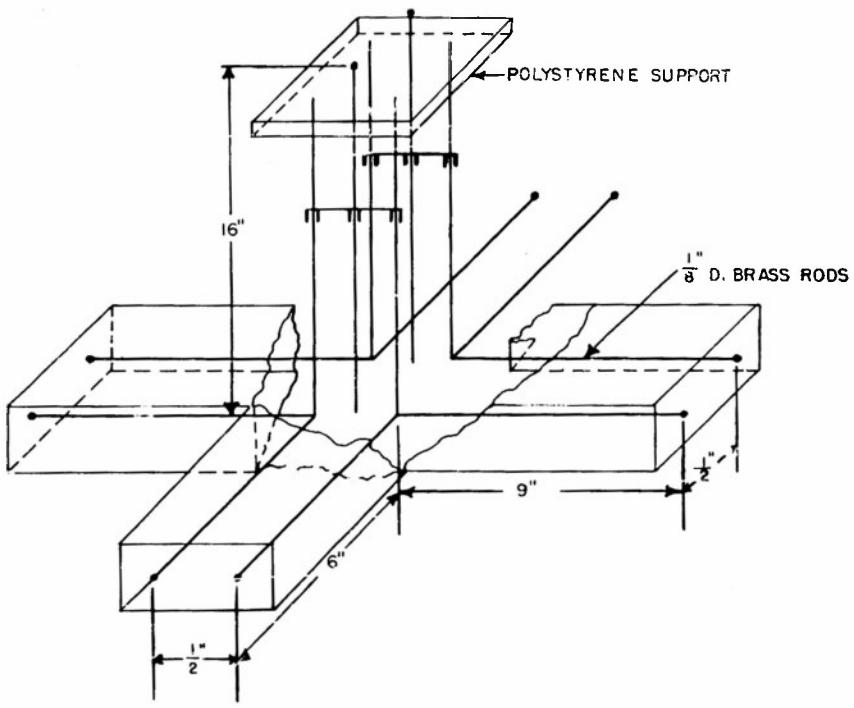

b

FIG. 2-1 SHIELDED TWO-WIRE HYBRID JUNCTION

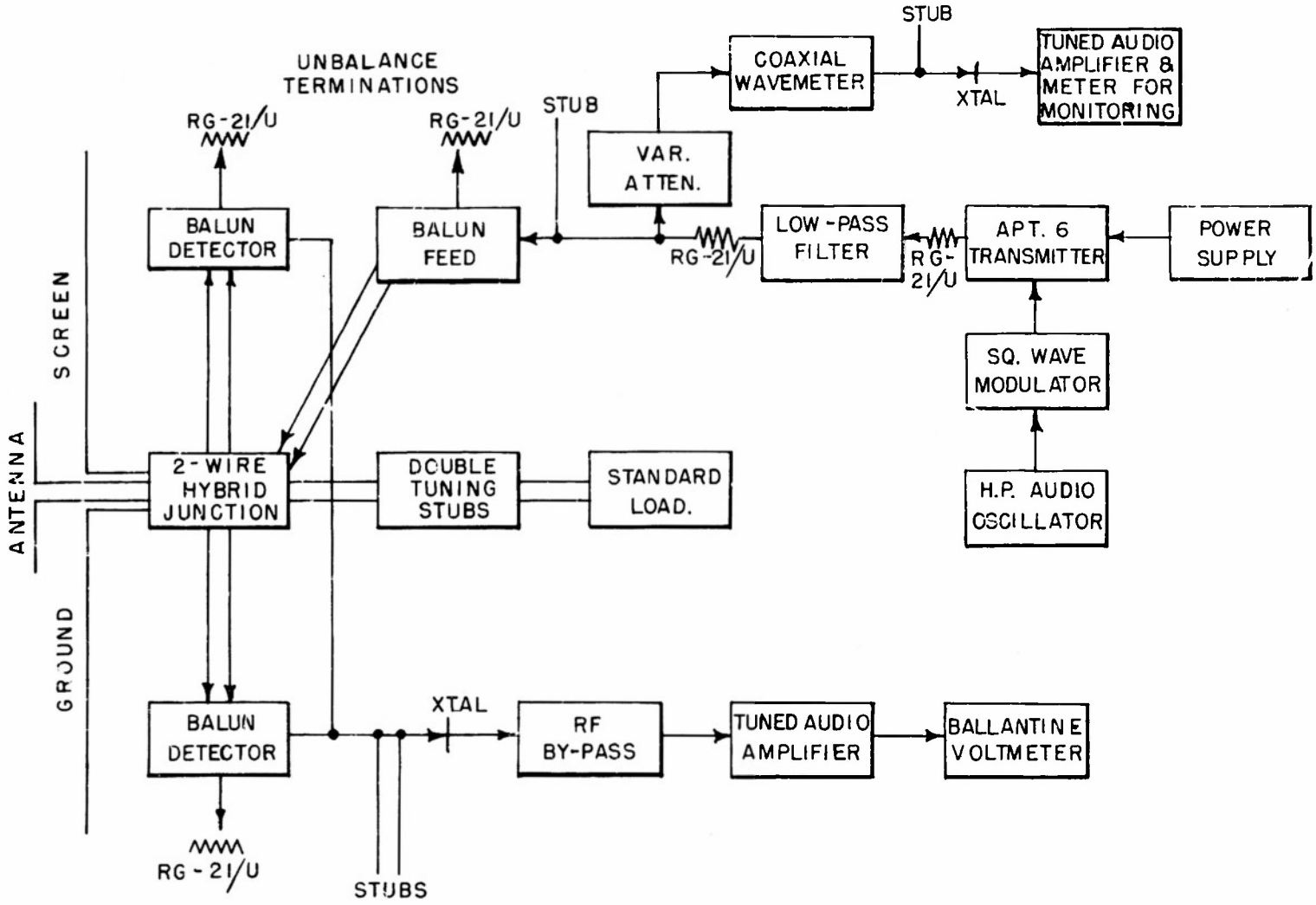

FIG. 2-2 IMPEDANCE BRIDGE BLOCK DIAGRAM

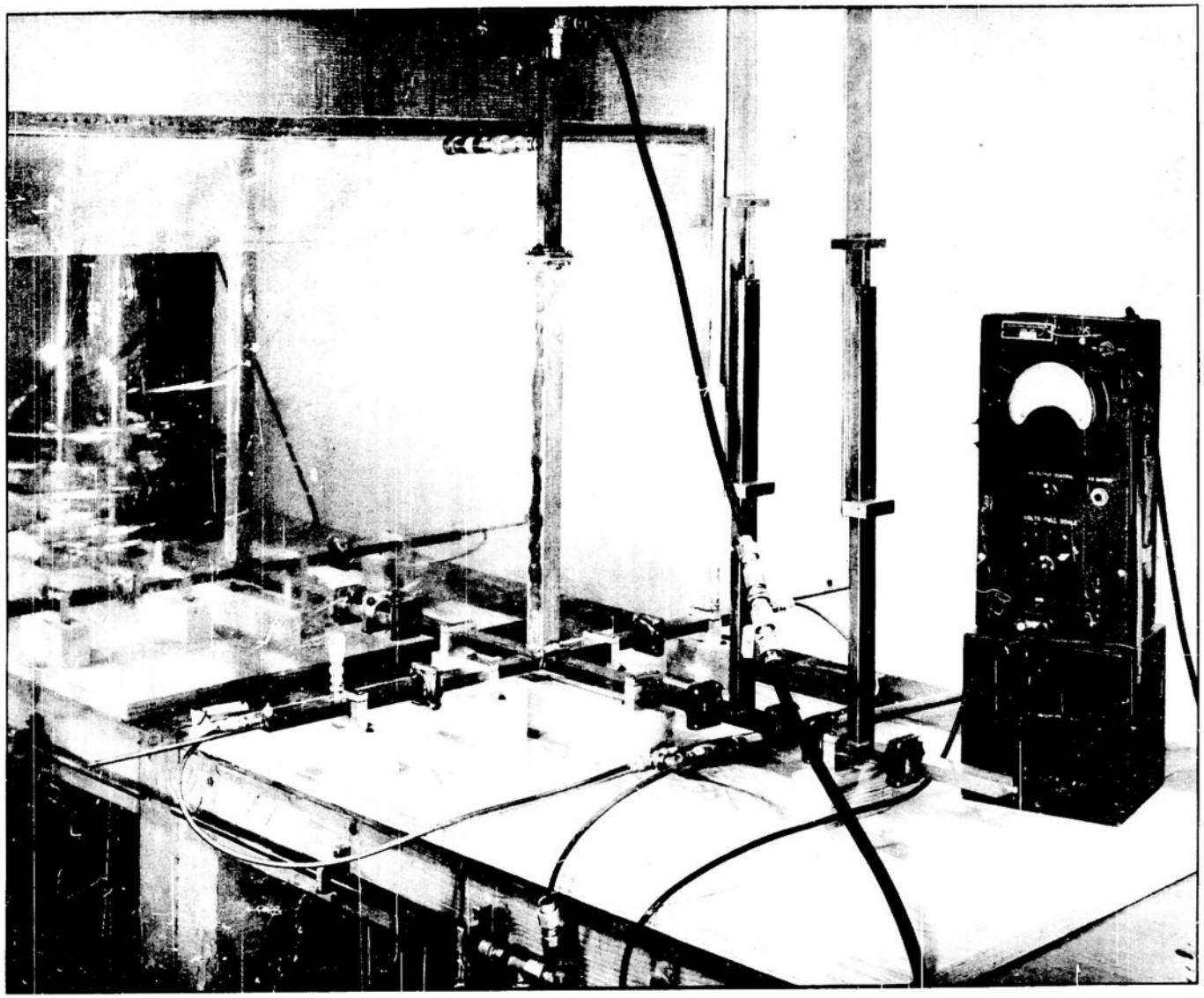

FIG. 2–3 TWO–WIRE IMPEDANCE BRIDGE

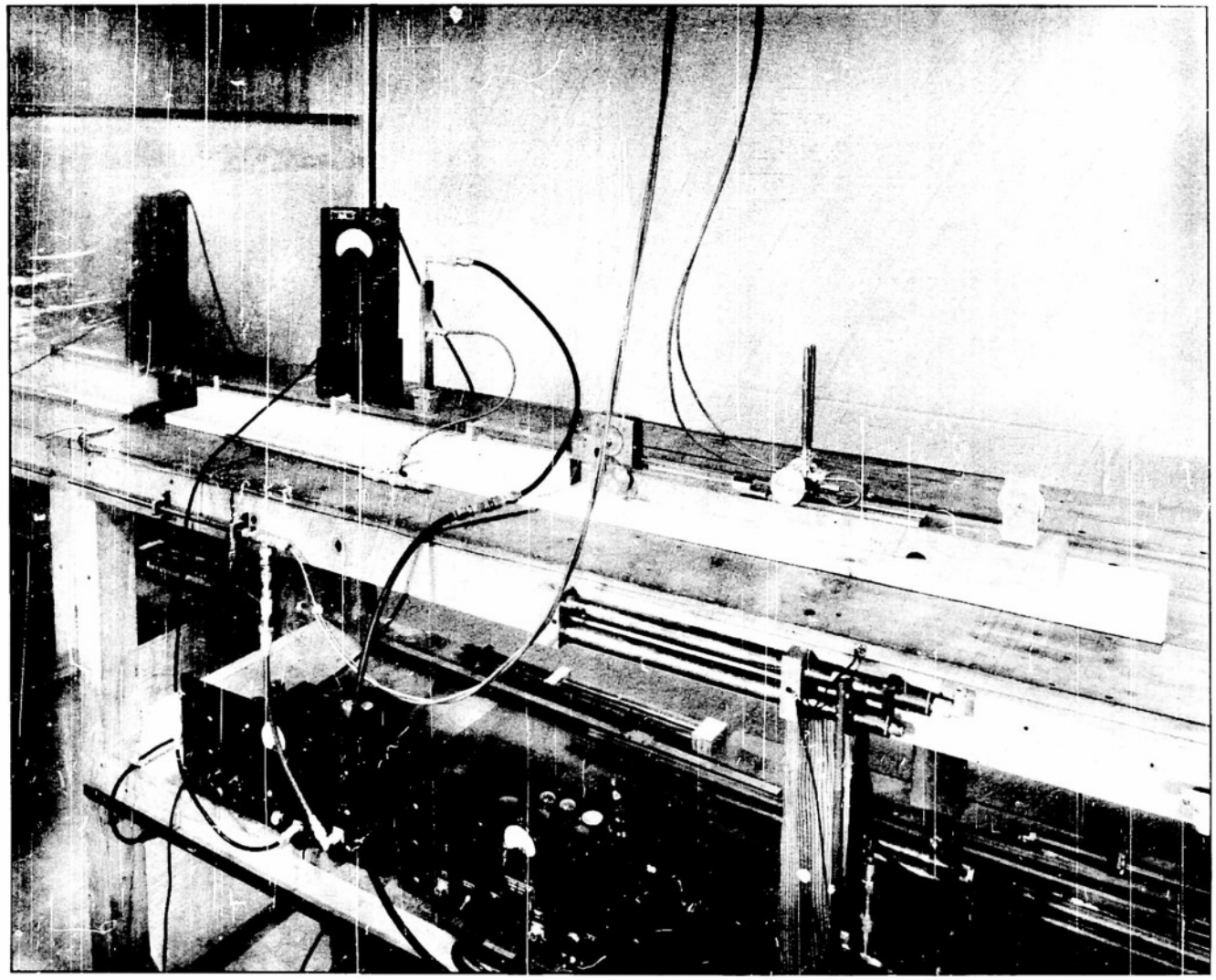

FIG. 2-4 SHIELDED TWO-WIRE SLOTTED LINE

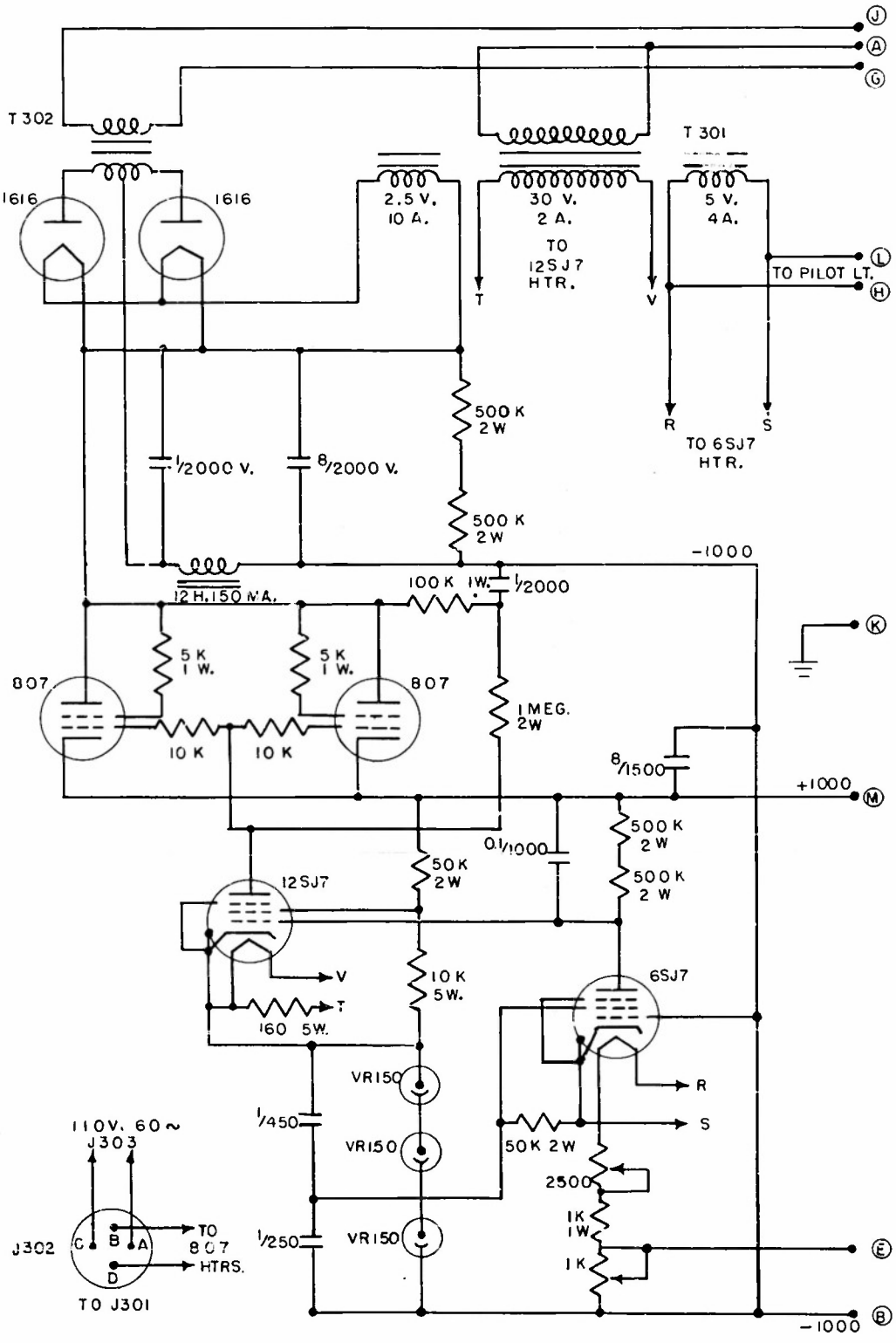

FIG. 2-5 TRANSMITTER, MODULATOR, AND POWER SUPPLY

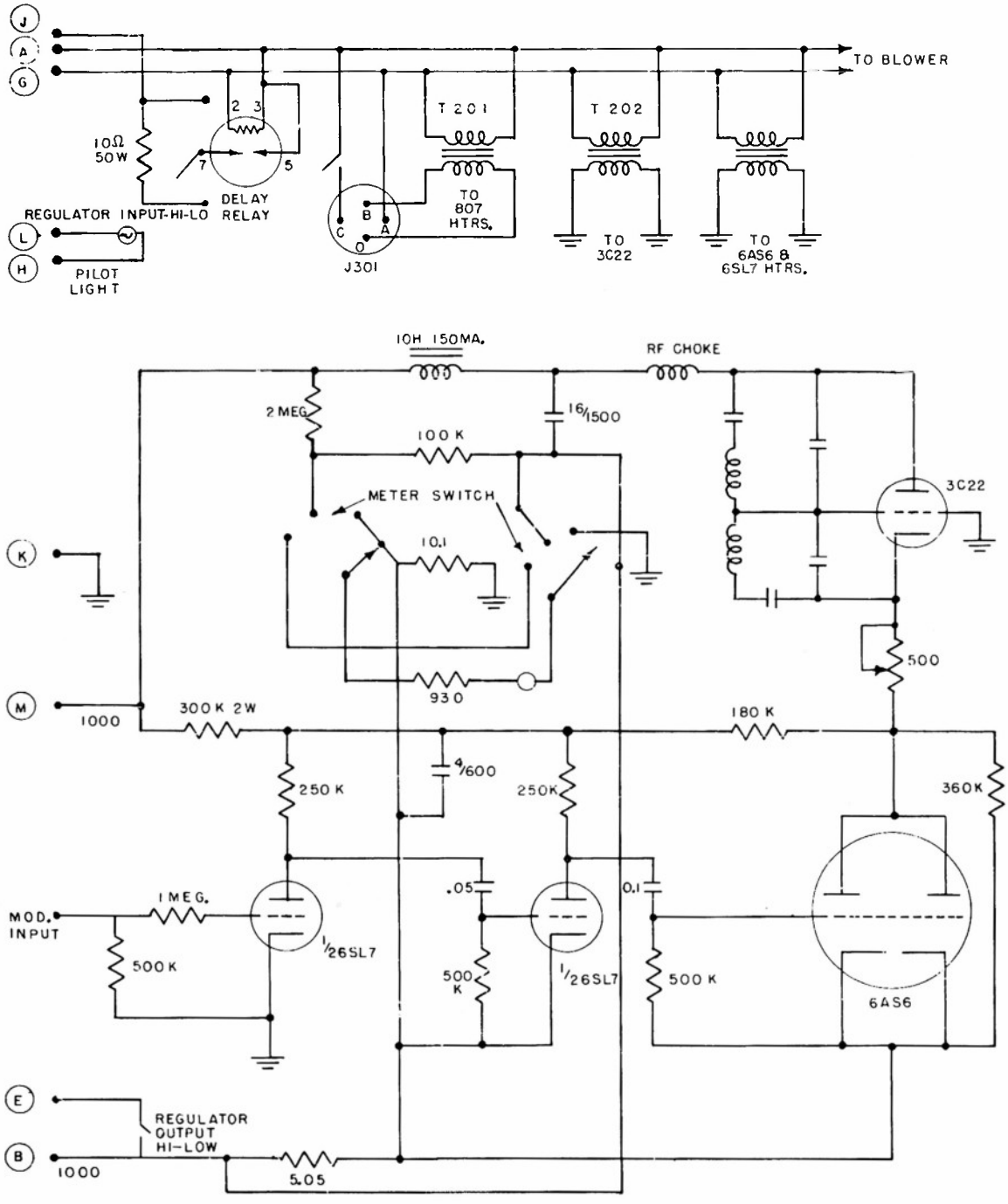
J
A
G
TO BLOWER
10Ω
50W
2 3
7
5
DELAY
RELAY
REGULATOR INPUT-HI-LO
L
H
PILOT
LIGHT
C
B
A
O
J301
T 201
TO
807
HTRS.
T 202
TO
3C22
TO
6AS6 &
6SL7 HTRS.
10H 150MA.
RF CHOKE
2 MEG
16/1500
100 K
METER SWITCH
3C22
K
10.1
500
930
M
1000
300 K 2W
180 K
4/600
250 K
250K
360K
.05
0.1
MOD.
INPUT
1 MEG.
500 K
1/26SL7
500
K
1/26SL7
500 K
6AS6
E
B
REGULATOR
OUTPUT
HI-LOW
1000
5.05

square wave is generated by an overdriven amplifier fed from a special Hewlett-Packard audio oscillator, for frequency stability. An earlier scheme for sinusoidal plate modulation was found to produce an objectionable amount of frequency modulation, effectively eliminated by the square-wave modulation.

Coaxial output from the transmitter is provided by a capacitive probe in the plate cavity, which is then fed through a 900-megacycle coaxial low-pass filter, padded on both sides by 10 db of lossy RG-21/U cable. The filter was incorporated to eliminate harmonics, as well as higher-mode oscillation of the transmitter at which the coaxial cavities are 3/4, 5/4, etc., wavelengths long. The filter was designed with ten sections, according to Cohn (8); it is shown in Fig. 2-6.

Frequency and amplitude monitoring of the transmitter were done using a coaxial wavemeter, crystal detector, and conventional tuned audio amplifier. Some difficulties were experienced with the coaxial wavemeter, apparently because of poor sliding contacts; consequently, final wavelength measurements were made on the two-wire slotted line.

Stray radiation from the transmitter, when objectionable, was reduced by enclosing the transmitter with bronze screening.

B. Detector

The detecting equipment consisted of a 1N21B crystal connected to a tuned 1000-cycle audio amplifier, whose output was read on a Ballantine a-c voltmeter. The circuit diagram of the amplifier is shown in Fig. 2-7. It incorporates a special tuned input transformer and tuned plate loads, all wound on high-Q (=100) toroids, plus a built-in regulated power supply.

The 1N21B crystal was held in a commercial holder designed for 10 cm operation, so it was found necessary to provide additional r-f filtering in the output line in the form of a 500 $\mu\mu$fd mica feed-through capacitor.

The crystal-amplifier combination was found to be accurately square-law for a range of at least 60 db in output voltage, above noise, provided saturation of the amplifier (beginning at about 5 volts) was not exceeded. This

range was found chiefly due to the special input transformer, whose low d-c resistance prevented self-biasing of the crystal. It was also found impossible to achieve square-law operation with low modulation levels of the transmitter, or with a modulation scheme employing a crystal driven at the modulation frequency. D-C biasing of the detector crystal was investigated, but found to decrease the overall signal-to-noise ratio, even though the signal could be increased up to 20 db.

C. Two-Wire Slotted Line

For impedance measurements using conventional standing-wave techniques (9), especially for calibration purposes, a shielded two-wire slotted line was constructed, as shown in Figs. 2-4 and 2-8. Its unique feature is the location of the electric-field-sampling probes, which extend outward through longitudinal slots in the line wires. These wires are 1/8-inch diameter hollow tubes through which a 1/16-inch diameter coaxial line slides for external connections to the probes. This arrangement is inherently better shielded and mechanically more stable than the frequently used probes projecting inward through slots in the shield (10).

One of the chief electrical problems encountered in the design of the slotted line was the elimination of discontinuities. For accurate impedance measurements on equipment with the same line configuration, it is necessary to minimize line discontinuities between the measured impedance and the point of measurement. Standard UG-39/U waveguide flanges were used to interconnect sections of the waveguide shield; these were found very satisfactory if reasonable care was taken to align them properly. Whenever possible, sections of line wires were screwed together; otherwise, sliding spring contacts had to be used. These were made by slotting the ends of the brass tubing, which was never completely satisfactory and continued to introduce errors into the measurements. The line wires in the slotted line were supported by a 4.75-inch section of polyfoam around the unslotted input section, a 1/4-inch section of polyfoam at the center of the slotted section, and solid polystyrene washers elsewhere beyond the slotted section; solid polyfoam was found undesirable around the entire slotted portion because it interfered with the probe travel. The dielectric constant of the

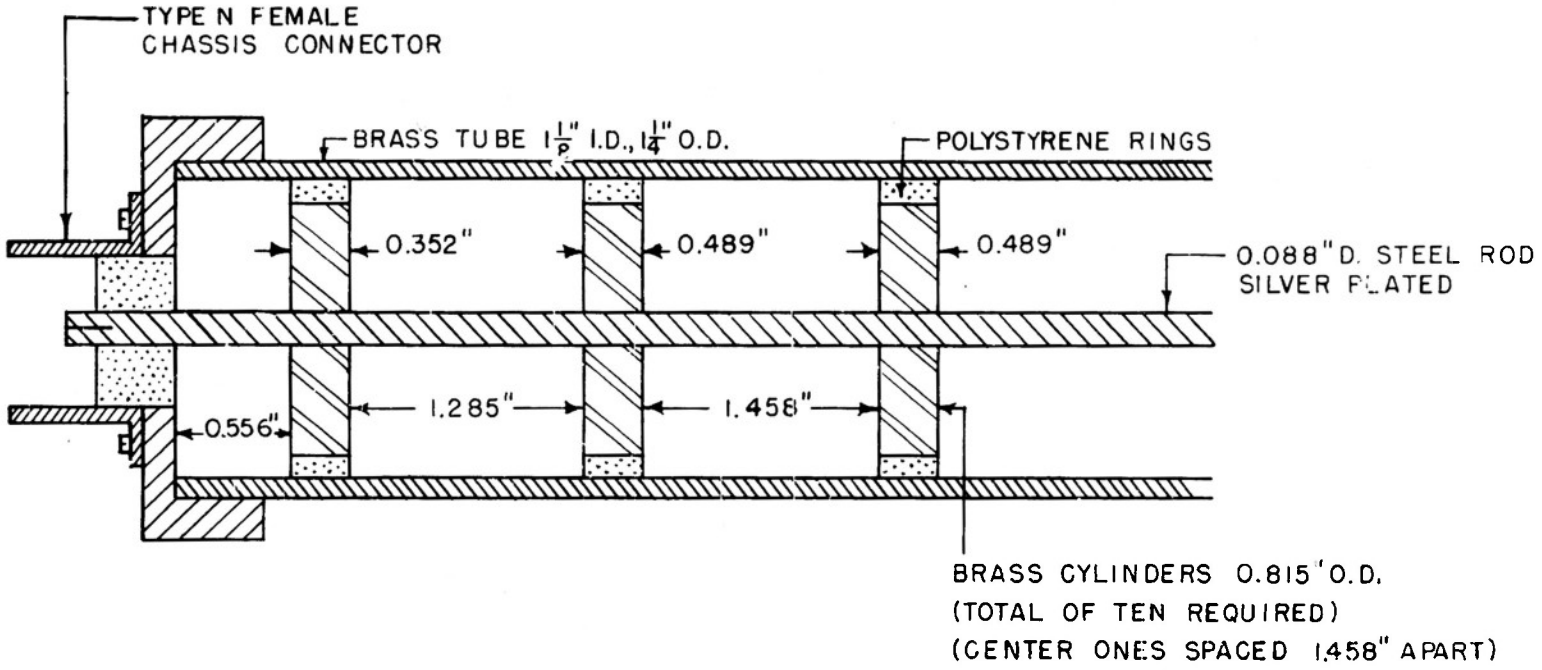

FIG. 2-6 900 mc. LOW PASS FILTER

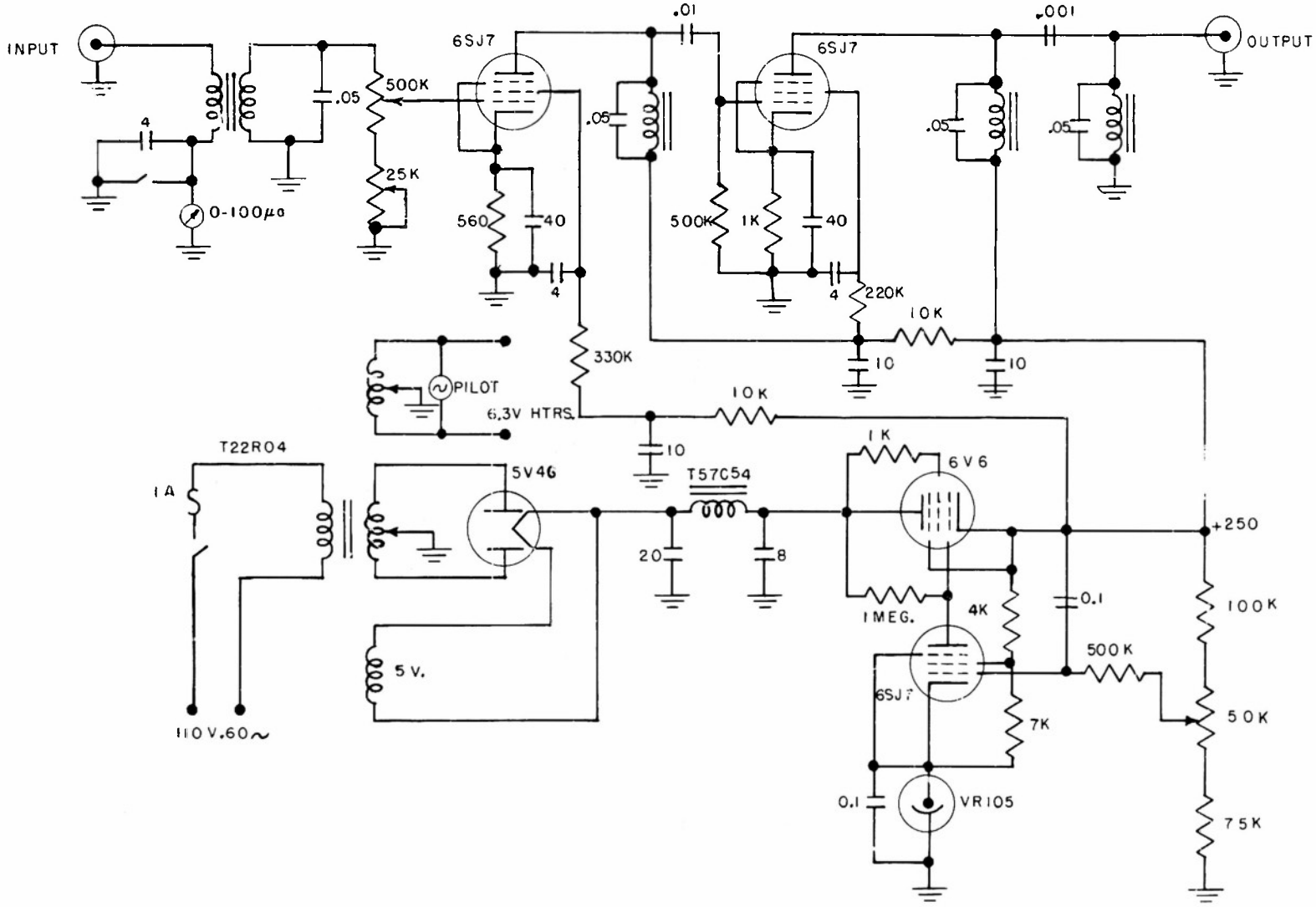

FIG. 2-7 TUNED AUDIO AMPLIFIER

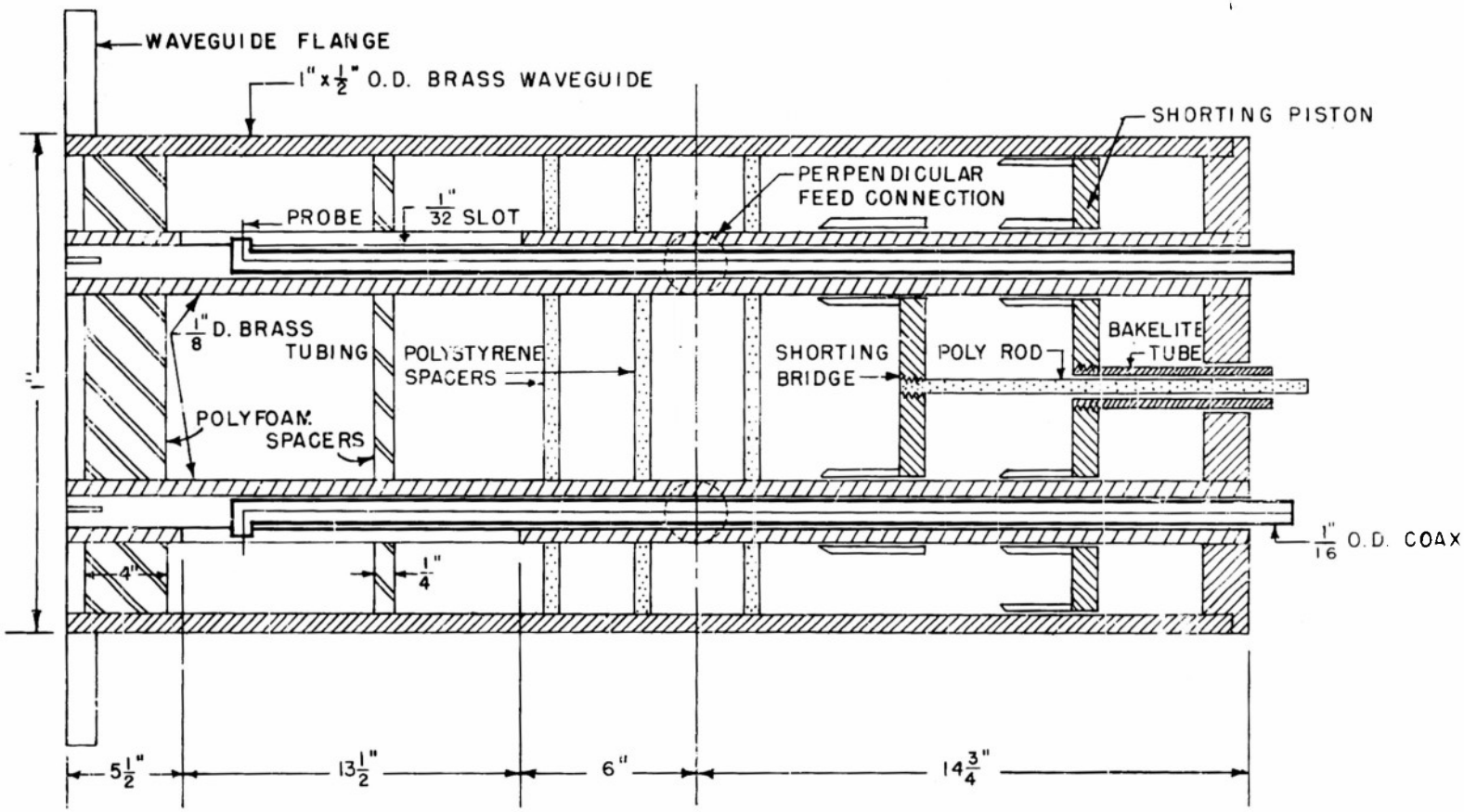

FIG. 2-8 SHIELDED TWO-WIRE SLOTTED LINE SCHEMATIC

polyfoam used was measured (by measuring the change which it produced in the electrical length of a section of line) and found to be 1.032; the discontinuity introduced by it is therefore negligible for most measurements. If maximum accuracy is desired, corrections can be made for the polyfoam by direct calculation of a 4.75-inch section of line with the appropriate dielectric constant. For large VSWR measurements, correction can be made by a slight shift in the observed position of the standing-wave minimum, as explained in Appendix A.

The probes consist of 0.013-inch wires protruding 1/16-inch from the line wires; it was not possible to detect any perturbation of the electromagnetic fields caused by the probes. Probe tuning was accomplished by a tuning stub at the end of each probe line, where flexible RG-56/U cables leading to the detector crystal were connected. The output from each probe is 35 to 40 db below the power level of the slotted line, indicating that larger probes could have been used without seriously disturbing the fields.

Measurements on the line were made by connecting the two probe outputs alternately to the same detector crystal, through a detachable Type-N connector, and averaging the two results. An SPDT coaxial switch available for this alternating connection was found unsatisfactory. Differences of more than 1 or 2 millimeters in the standing-wave positions, or 1 or 2 db in the standing-wave ratios on the two lines, were ascribed to the presence of unbalanced currents; such measurements were discarded, and an attempt to locate the source of the unbalance was made before repeating such measurements.

The slotted line can be used for the measurement of balanced and unbalanced currents simultaneously, if desired, described in Technical Report 183. In order to avoid phase measurements, it was found necessary to eliminate one mode from the incident wave; this is conveniently accomplished with the balun feed described previously, which also facilitates proper termination of both reflected waves.

D. Coaxial Slotted Line

For measurement of the characteristics of the balance-unbalance detectors, as described in Chapter I, it was necessary to build a coaxial slotted line, whose constructional details are shown in Figs. 2-9, -10, -11, and 12. With the purpose in mind of building an instrument which could be used for other laboratory measurements, it was designed to operate over the frequency range 200 to 1000 Mc/s, and mounted on a 12-foot aluminum I-beam for portability. The measuring line proper consists of a 7/8-inch inside diameter brass tube surrounding a 3/8-inch outside-diameter brass tube, separated by a continuous set of polyfoam spacers, giving a characteristic impedance of 50.1 ohms. The probe extends outward through a slot in the inner tube, and is positioned as well as connected to the detector circuit by a 5/16-inch outside-diameter coaxial line which slides inside the 3/8-inch tube. Probe details are shown in Fig. 2-11. In order to minimize discontinuities between the slotted line and the apparatus on which measurements are to be made, a 13-inch tapered section is provided for connection to a Type-N connector, as shown in Fig. 2-10.

III

EXPERIMENTAL RESULTS OF BRIDGE OPERATION

A. Measuring Setup

Actual measurements using the impedance bridge result in answers which are normalized with respect to the characteristic impedance of the shielded two-wire line used throughout the equipment, and which are referred to a plane the same distance from the center plane of the hybrid junction as the reference plane of the input stub of the standard load. If the impedance to be measured is located other than at this reference plane, it will have to be related to the measured result in some way such as by transformation along a length of connecting transmission line, taking proper care to account for any discontinuities. In particular, for measurements on radiating antennas fed from an open two-wire line, the impedance bridge shield will have to be terminated and the measurements corrected accordingly. Such a

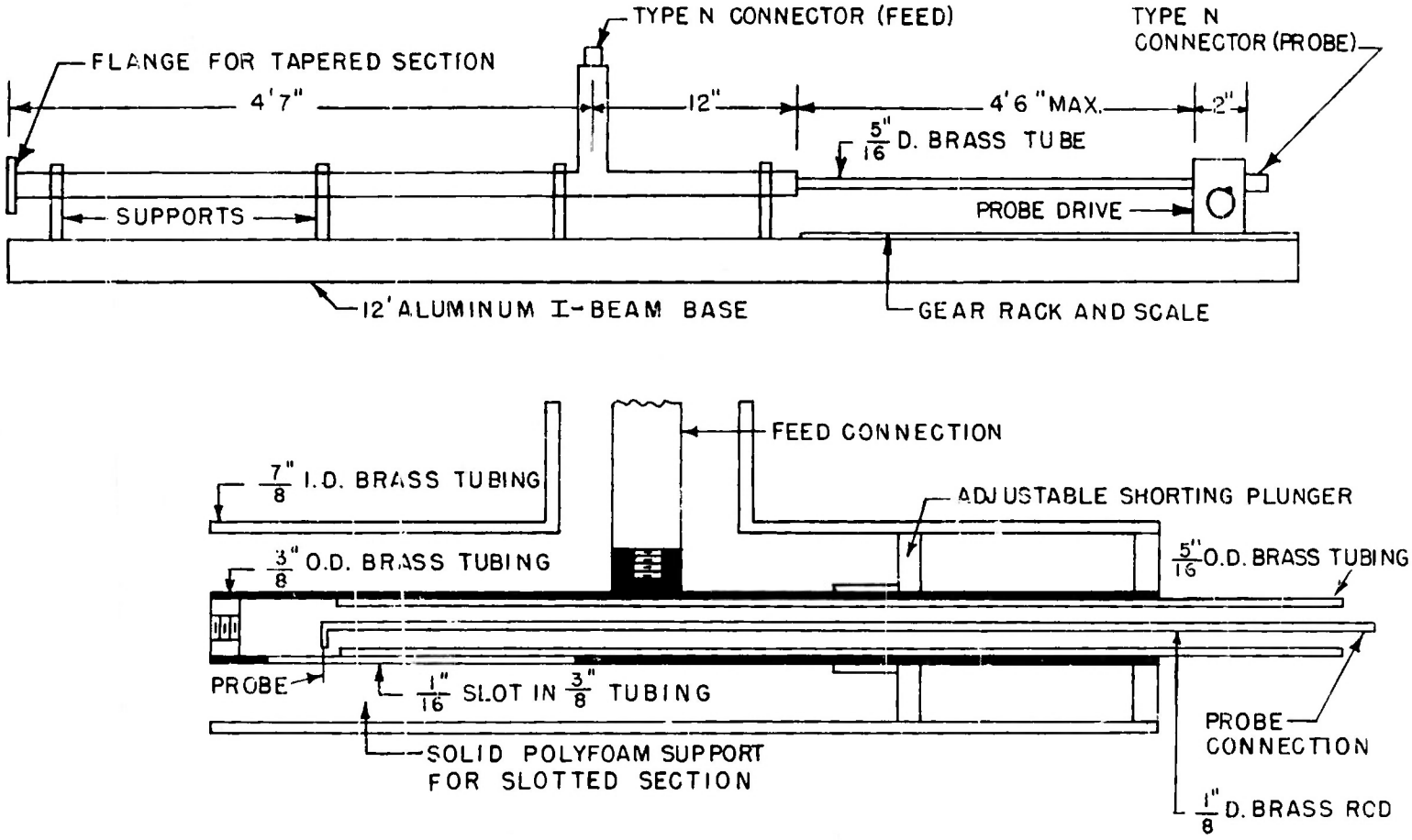

FIG. 2-9 COAXIAL SLOTTED LINE

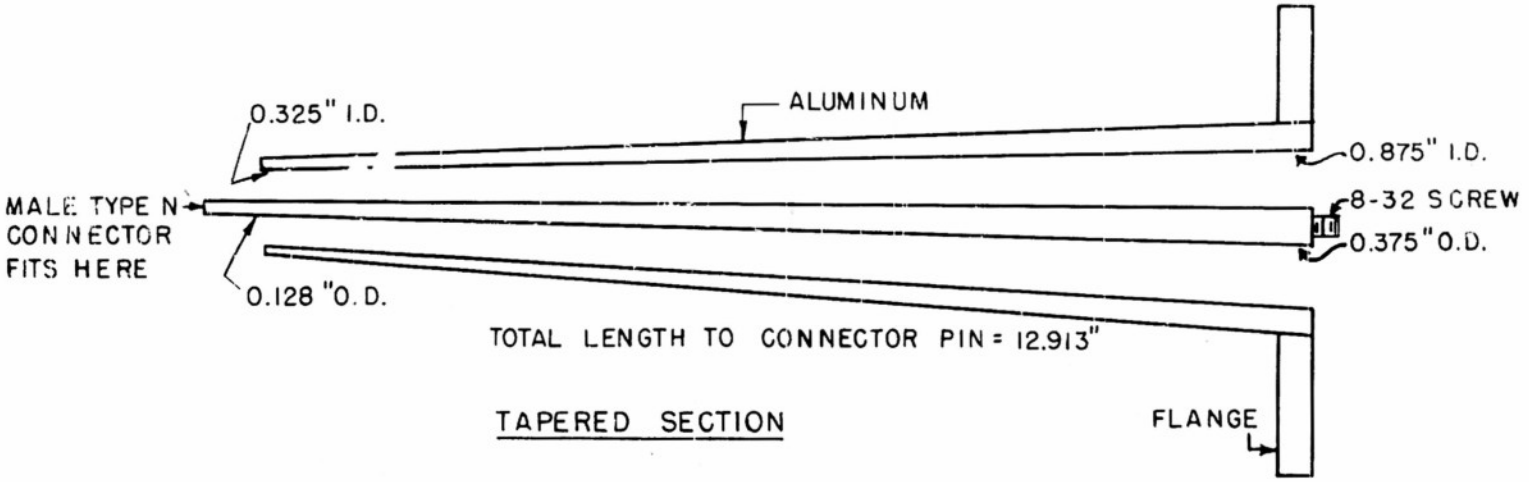

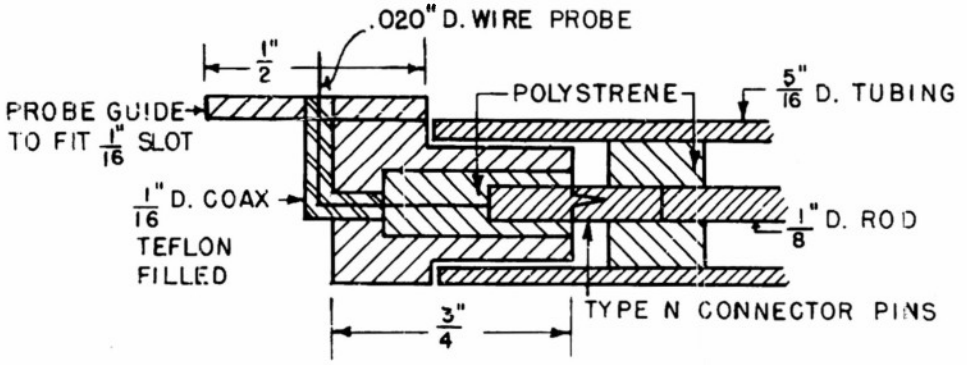

PROBE DETAIL

FIG. 2-10 COAXIAL SLOTTED LINE COMPONENTS

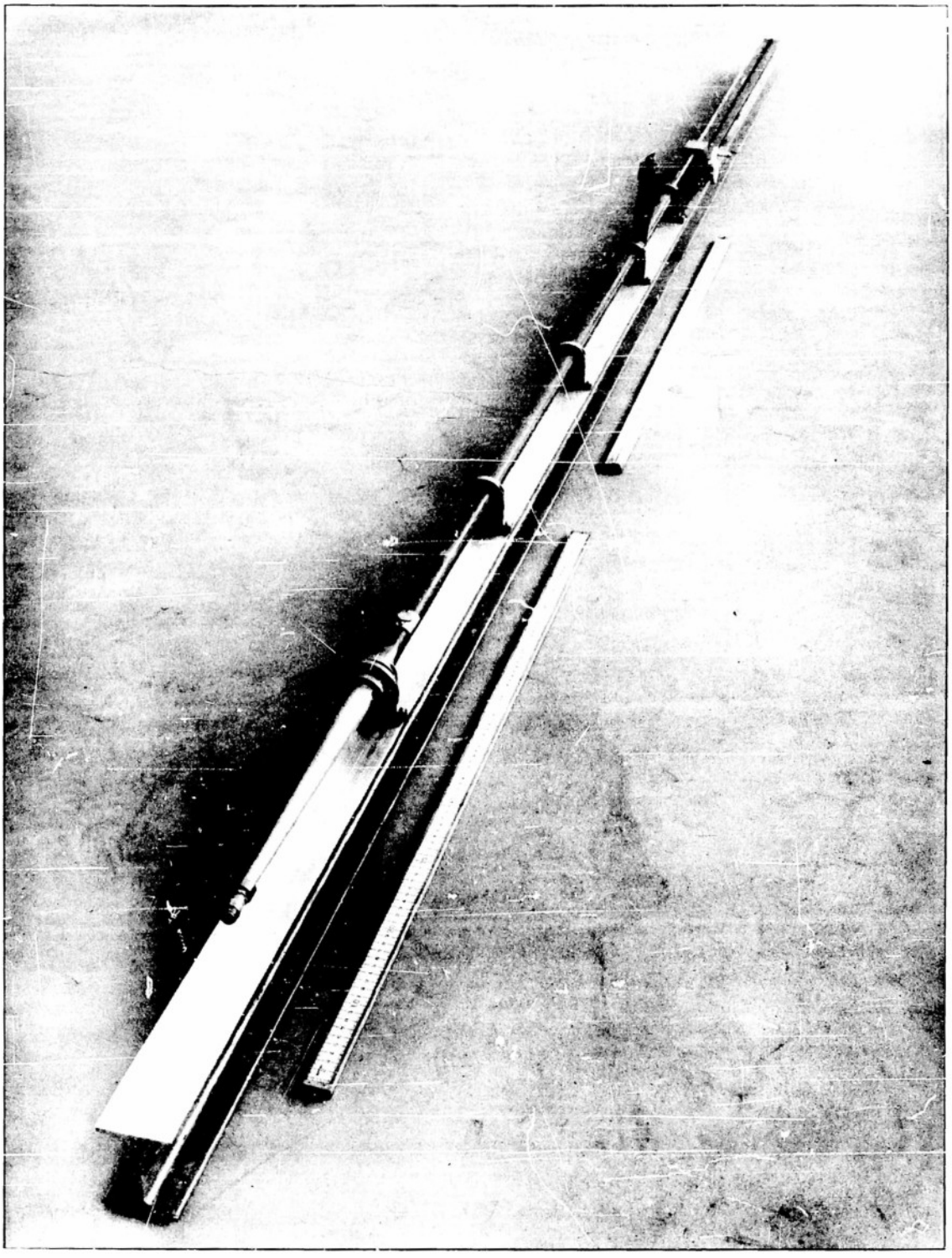

FIG. 2—11 COAXIAL SLOTTED LINE

correction is inevitable if the operator and measuring equipment are to be shielded from the structures being measured; the only alternative is to use one wire over an image plane, as done by Conley (11), in which case structures which are asymmetric to the image plane cannot be measured.

In order to test the operation of the bridge and associated equipment, it was decided to measure a number of impedances which could be checked by the conventional slotted-line method. Measurements were made on a series of antennas fed from an open two-wire line, and the transition from the shielded line was made by terminating the shield on a ground screen. This ground screen consisted of a 3/32-inch aluminum sheet 44 x 48 inches, with extensions of bronze screening approximately three feet below and five feet above the aluminum sheet, as shown in Figs. 2-3, 2-4, and 3-1. No corrections for the ground screen are needed to check the bridge measurements against those made on the slotted line, as the comparisons may be made at some plane within the shielded line. However, to find the actual antenna impedances at the plane of the antenna, four corrections are necessary, as follows:

(1) Ground Screen Transition

The transition from shielded line to open line may be considered a two-terminal-pair network, and analyzed as such by Deschamps' Method (4). Measurements were made on the slotted line of the input reflection coefficient as a function of position of a short circuit consisting of a tandem bridge on the open line. The results of these measurements agree extremely well with an assumed equivalent circuit consisting of a shunt capacitance and a simple discontinuity in characteristic impedance, yielding a value of 0.1414 $\mu\mu$fd for the capacitance, or 1525 ohms at 738.2 Mc/s.

(2) Difference in Characteristic Impedance

The antennas were connected on the end of a 12-inch section of open two-wire line consisting of 1/8-inch diameter brass rods, the same as used in the shielded sections, supported by a large block of polyfoam. The characteristic impedance of this open-wire section is given by (12).

$$Z_c = \frac{120}{\sqrt{\epsilon}} \cosh^{-1} \frac{b}{2a} = \frac{120}{1.016} \cosh^{-1} 4 = 241.65 \text{ ohms}$$

Impedances measured at the ground screen, after correction for the ground screen transition, will have to be transformed along a 12-inch section of transmission line with this characteristic impedance.

(3) Terminal Effects

The actual antenna impedance measured differs from the theoretical impedance Z_δ of an idealized linear antenna driven from a finite gap of length 2δ because of the capacitive coupling between the antenna and the transmission line, and because of the variation in line parameters near the end of the line where the antenna is connected (6). These effects are confined chiefly to a terminal zone of length approximately 10b , where b is the line spacing; and for small values of b such that the terminal zone is a small fraction of a wavelength, these terminal effects may be lumped into an equivalent inductance L_T in series with the antenna and a capacitance C_T in shunt. The apparent terminal admittance Y_{sa}, which is the actual admittance seen one-half wavelength from the antenna, is thus related to the antenna impedance Z_δ by

$$Z_\delta = \frac{1}{Y_{sa} - j\omega C_T} - j\omega L_T \qquad (3\text{-}1)$$

where L_T and C_T for the line used are found to be (6)

$$L_T = -\frac{(b-a)}{2\pi \nu_o} = -.00222 \text{ microhenries}$$

$$C_T = -0.67\, b c_o = -0.67\, b \frac{\pi \epsilon_o}{\cosh^{-1} \frac{b}{2a}} = -0.115 \mu\mu\text{fd} \qquad (3\text{-}2)$$

At 738.2 Mc/s, $X_{L_T} = -j\,10.30$ ohms and $X_{C_T} = j\,1875$ ohms.

(4) Image Effect

Radiation from the antenna under test will be reflected from the ground screen and interact with currents on the antenna to produce the same effect as an image of the original antenna, located an equal distance behind the ground screen, and coupled inductively to the original. The measured antenna impedance will thus be the isolated antenna impedance modified by some coupling term. The antennas actually measured consisted of a number of types of multiple folded dipoles nearly a half-wavelength

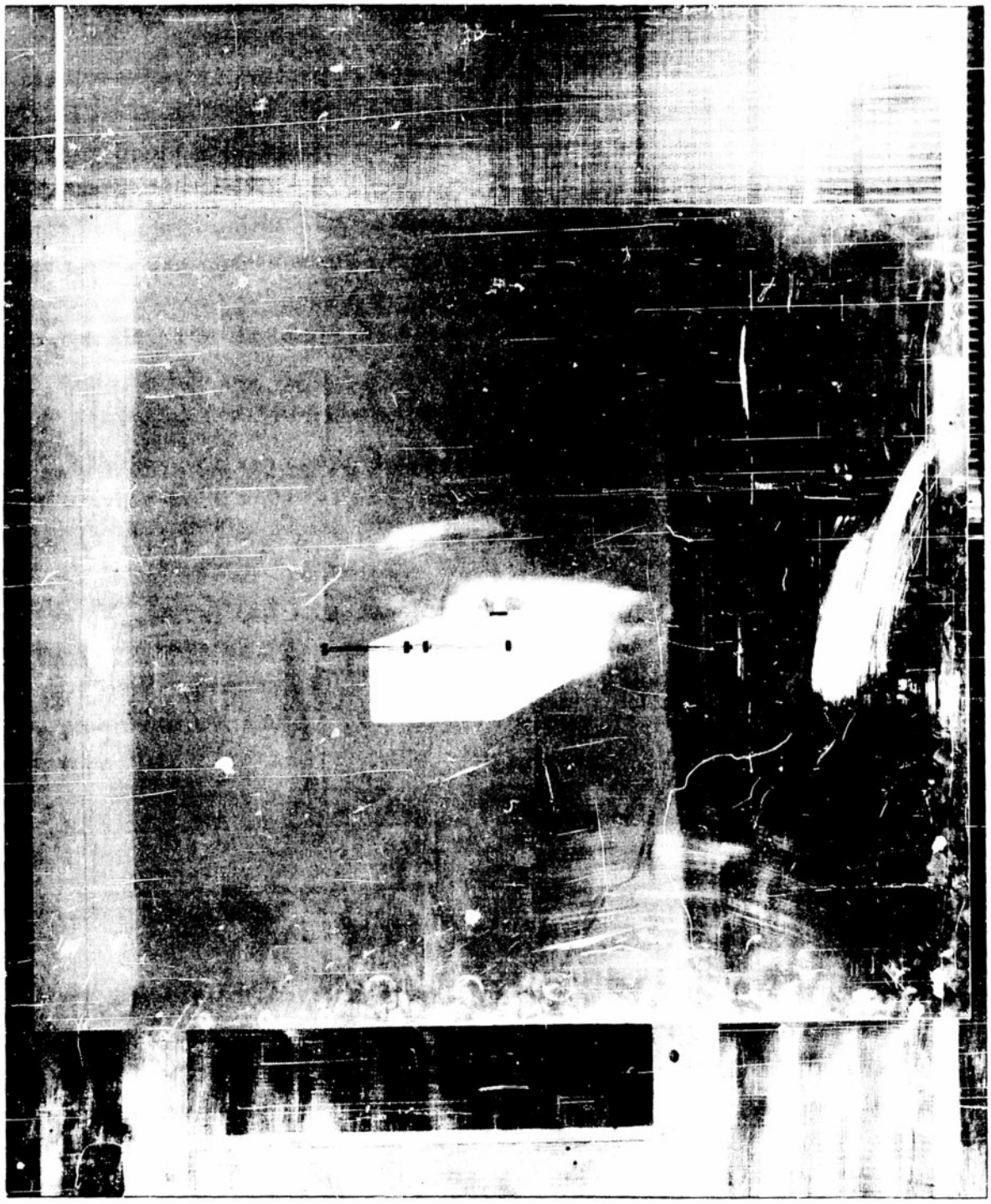

FIG. 3--1 ANTENNA AND GROUND SCREEN

long; the currents on these folded dipoles consist of nonradiating transmission-line components, plus radiating components equivalent to those of a simple dipole of modified radius. The coupling correction for a simple dipole with this modified radius may be applied to these folded dipoles without excessive error. Naturally, the smaller the coupling term becomes, the smaller will be the error in the calculated antenna impedance due to the use of this simple dipole coupling correction. On the other hand, when the antenna is located farther from the ground screen in order to reduce coupling to its image, the effect of the finite ground screen becomes greater, so that the simple image theory is no longer valid. A compromise was reached by locating the antenna twelve inches from the ground screen.

For two driven coupled antennas, designated by subscripts 1 and 2, the driving-point voltages and currents are related by

$$V_1 = I_1 Z_{s1} + I_2 Z_{12} \qquad V_2 = I_1 Z_{21} + I_2 Z_{s2} \qquad (3\text{-}3)$$

where Z_{s1} is the self-impedance of antenna 1 in the presence of antenna 2, with the generator on antenna 2 open-circuited ($I_2 = 0$); and similarly for Z_{s2}. By reciprocity, $Z_{12} = Z_{21}$, representing the mutual impedance between antennas 1 and 2. For the case where antenna 2 is the image of antenna 1, $I_2 = -I_1$, and

$$V_1 = I_1(Z_{s1} - Z_{12})$$

or

$$\frac{V_1}{I_1} = Z_1 = Z_{s1} - Z_{12} \qquad (3\text{-}4)$$

where Z_1 is the measured antenna impedance Z_{sa} modified by the terminal network involving L_T and C_T. (This terminal network will be unaffected by coupling to the image because of the relative distances involved.) The self-impedance of the antenna, $Z_{s1} = Z_1 + Z_{12}$ can thus be calculated if Z_{12} is known. This self-impedance in the presence of the open-circuited image will be practically the same as the self-impedance of an isolated antenna, because of the relatively large separation and the fact that the open-circuited image becomes two collinear quarter-wave

dipoles, which have only small currents induced in them.

The analysis of two parallel identical antennas was carried out by King and Harrison (13) and later improved by Tai (14), who evaluated the current distributions and self- and mutual-impedances of half-wave and full-wave dipoles with three values of radii for separations up to one wavelength. His computations lead to so-called first-order results, since they account for terms in the King-Middleton (15) series expansion up to the first order. Tai's computations were extended in range of antenna lengths and radii, and further improved by an approximate second-order theory, by King (16). These results verify the previous assertion that the self-impedance in the presence of the image is very nearly the same as the isolated self-impedance. Unfortunately, the range of separations evaluated in the above references is from zero to one wavelength, while the separation used in the present measuring setup is 1.5 wavelengths. Consequently, the only numerical results which are available for this spacing are zero-order values for very thin half-wave dipoles; these, however, agree quite well with higher-order values for spacings greater than one wavelength. For $3\lambda/2$-spacing, this zero-order value is $Z_{12} = -1.89 - j12.30$ ohms (6) for half-wave dipoles only. An approximate value for slightly different lengths may be obtained by modifying this value in accordance with the variation as a function of length calculated by King for somewhat smaller spacings (16, Fig. 16). It is apparent that the resistive component is fairly constant, while the reactive component for a spacing of $\beta_o b = 5$ varies as follows:

$\beta_o h$	$X_{12}(\beta_o b=5)$	$X_{12}(b=3\lambda/2)$
1.25	5.5	-3.9
1.33	7	-4.9
1.41	10	-7.0
1.49	13.5	-9.5
1.57	17.5	-12.3
1.64	23	-16.2
1.72	28	-19.7

Here the value for $3\lambda/2$ spacing is computed proportionately.

The application of this correction term to a folded dipole may be examined as follows. If subscripts 1 and 2 are used again to denote the actual and the image antennas, respectively, and primes to denote quantities pertaining to the parasitic element of each, the following general relation is valid:

$$V_1 = I_1 Z_{s1} + I_{1'} Z_{11'} + I_2 Z_{12} + I_{2'} Z_{12'} \tag{3-5a}$$

$$0 = I_1 Z_{11'} + I_{1'} Z_{s1} + I_2 Z_{1'2} + I_{2'} Z_{1'2'} \tag{3-5b}$$

Because of the relative distances and the definition of an image, $I_1 = -I_{2'}$, $I_{1'} = -I_{2'}$, and $Z_{12} = Z_{1'2'} = Z_{1'2} = Z_{12'}$.

$$V_1 = I_1(Z_{s1} - Z_{12}) + I_{1'}(Z_{11'} - Z_{12}) \tag{3-6a}$$

$$0 = I_1(Z_{11'} - Z_{12}) + I_{1'}(Z_{s1} - Z_{12}) \tag{3-6b}$$

$$Z_1 = \frac{V_1}{I_1} = Z_{s1} - Z_{12} - \frac{(Z_{11'} - Z_{12})^2}{Z_{s1} - Z_{12}} \tag{3-7}$$

According to the method of symmetrical components, Z_{s1} and $Z_{11'}$ may be written as: (6)

$$Z_{s1} = \frac{1}{2}(Z^s + Z^a) \qquad Z_{11'} = \frac{1}{2}(Z^s - Z^a) \tag{3-8}$$

where Z^s is the input impedance of the isolated folded dipole with symmetrical generators in each element; and Z^a is the corresponding impedance with anti-symmetrical generators. Then,

$$Z_1 = \frac{(Z^s + Z^a - 2Z_{12})^2 - (Z^s - Z^a - 2Z_{12})^2}{2Z^s + 2Z^a - 4Z_{12}} \tag{3-9}$$

$$= \frac{2Z^s Z^a - 4Z_{12}Z^a}{Z^s + Z^a - 2Z_{12}} = \frac{2Z^s - 4Z_{12}}{1 + \dfrac{Z^s - 2Z_{12}}{Z^a}}$$

If the two elements of the folded dipole are closely spaced, the anti-

symmetrical case approaches a balanced transmission line; and for $\beta_o h = \pi/2$, $Z^a \longrightarrow \infty$, and $Z_1 \longrightarrow 2Z^s - 4Z_{12}$. This relation is valid so long as $[(Z^s - 2Z_{12})/(Z^a)]^2 << 1$, which is substantially true for the range of antenna lengths measured. The input impedance of an isolated folded dipole will thus be the measured impedance Z_1 increased by $4Z_{12}$, where Z_{12} is the coupling term for simple dipoles. By analogy, the additive correction term for folded tripoles will be $9Z_{12}$, and for folded quadrupoles $16Z_{12}$.

B. Antenna Measurements

Impedance measurements were made on the shielded two-wire bridge for seven different lengths, centering around a half-wavelength, of each of four types of antennas, including simple dipoles, folded dipoles, and what will be called folded tripoles and folded quadrupoles, as illustrated in Fig. 3-2. The last two types of antennas were measured in order to verify theoretical calculations by Charles W. Harrison, Jr. (17). Measurements of the first three types of antennas were repeated on the two-wire slotted line for comparison purposes. Results of these measurements are given in Table 3-1, and plotted in Figs. 3-3 and 3-4. Antenna characteristics are given in Appendix B.

Agreement between measurements using the two methods is seen to be very good for simple dipoles, but not quite so good for folded dipoles and tripoles. The reasons for this are believed to be as follows: first, as the magnitude of the impedances under measurement departs from the characteristic impedance of the measuring line, accuracy naturally decreases, because of the critical adjustment required of the standard. Second, the actual antennas were composed of sections which were screwed together, some of the sections being used in common for all of the antennas, to avoid unnecessary duplication of parts. Furthermore, the individual elements of the multi-element antennas were held apart by somewhat flimsy spacers of a vinyl-plastic foam-type material, to maintain relatively constant spacing without introducing appreciable dielectric discontinuity (the dielectric constant of the vinyl-foam is reported to be 1.07). Because of the difficulty of changing from one measuring setup to the other, all measurements were

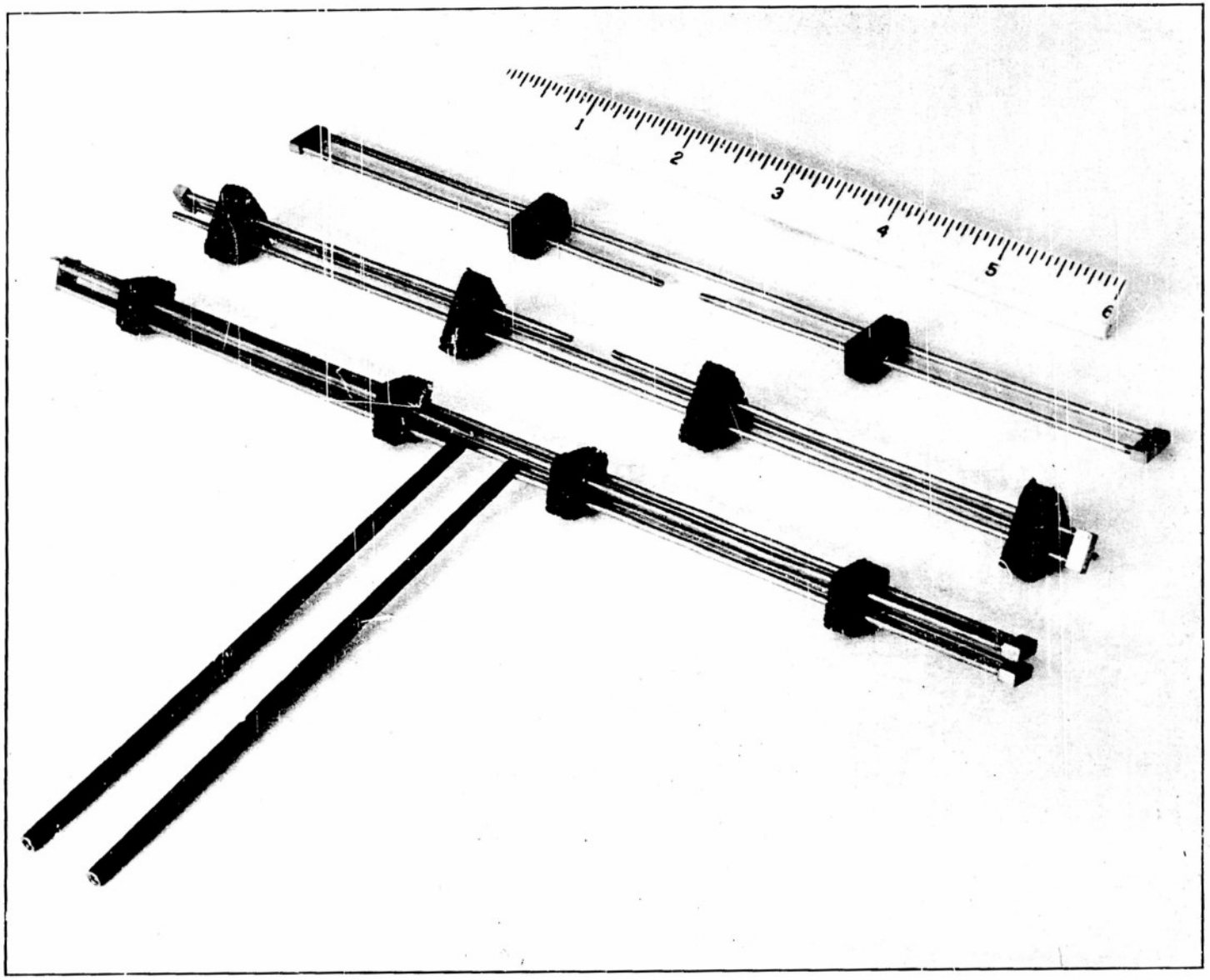

FIG. 3-2 ANTENNA CONFIGURATIONS

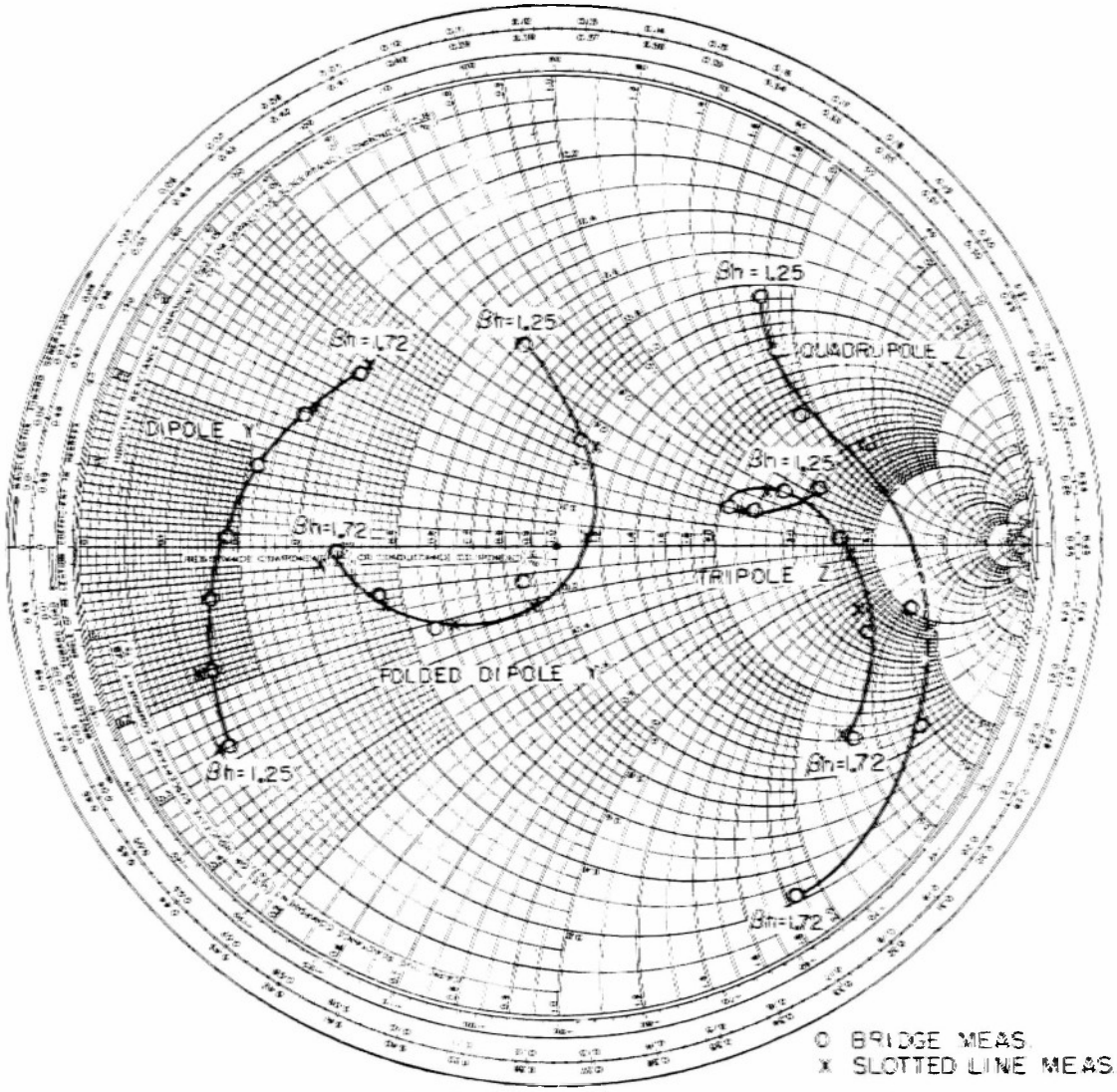

FIG. 3-3a RESULTS OF ANTENNA MEASUREMENTS
(EVALUATED AT BRIDGE REFERENCE PLANE)

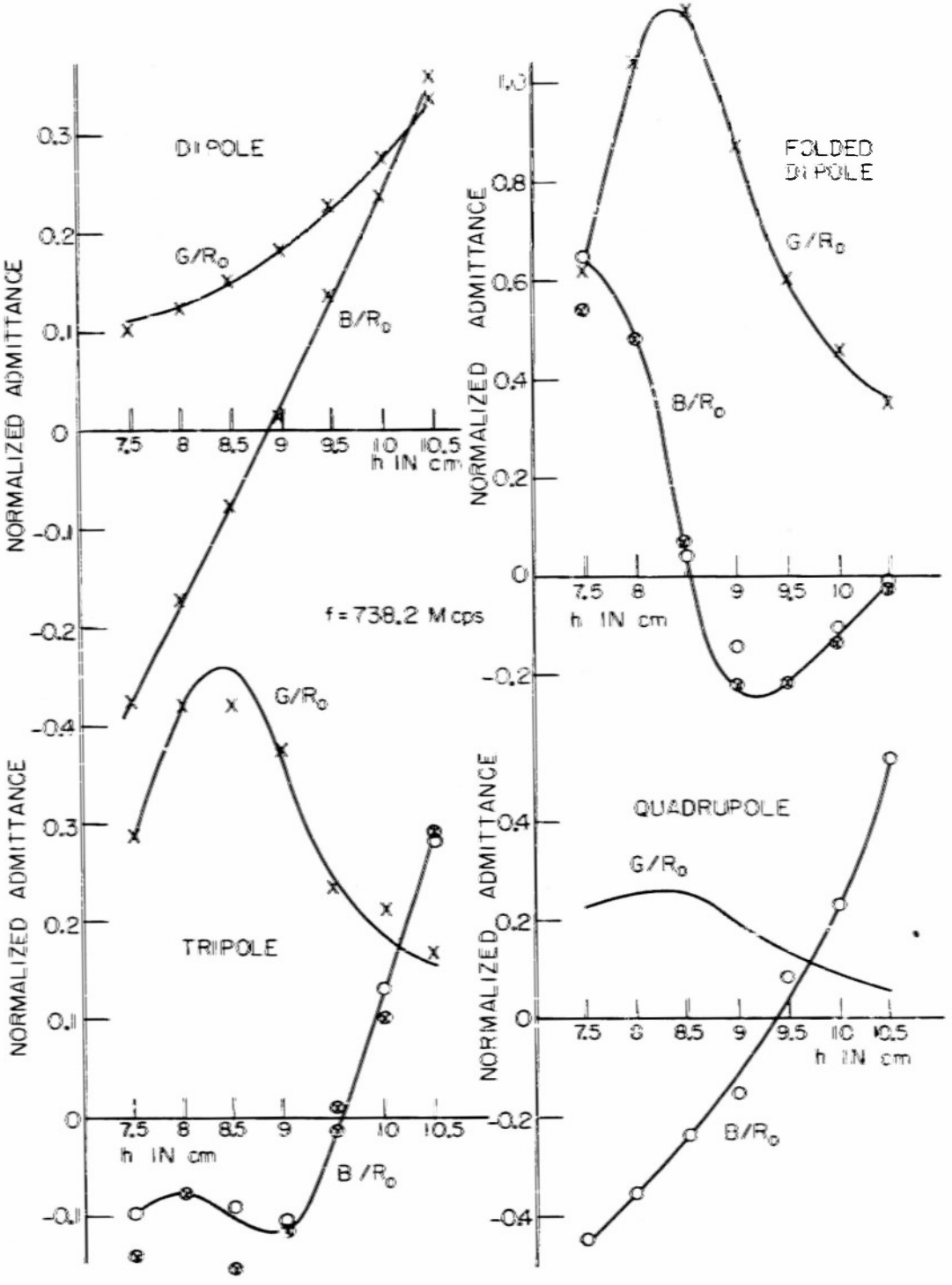

FIG. 3-3b RESULTS OF ANTENNA MEASUREMENTS

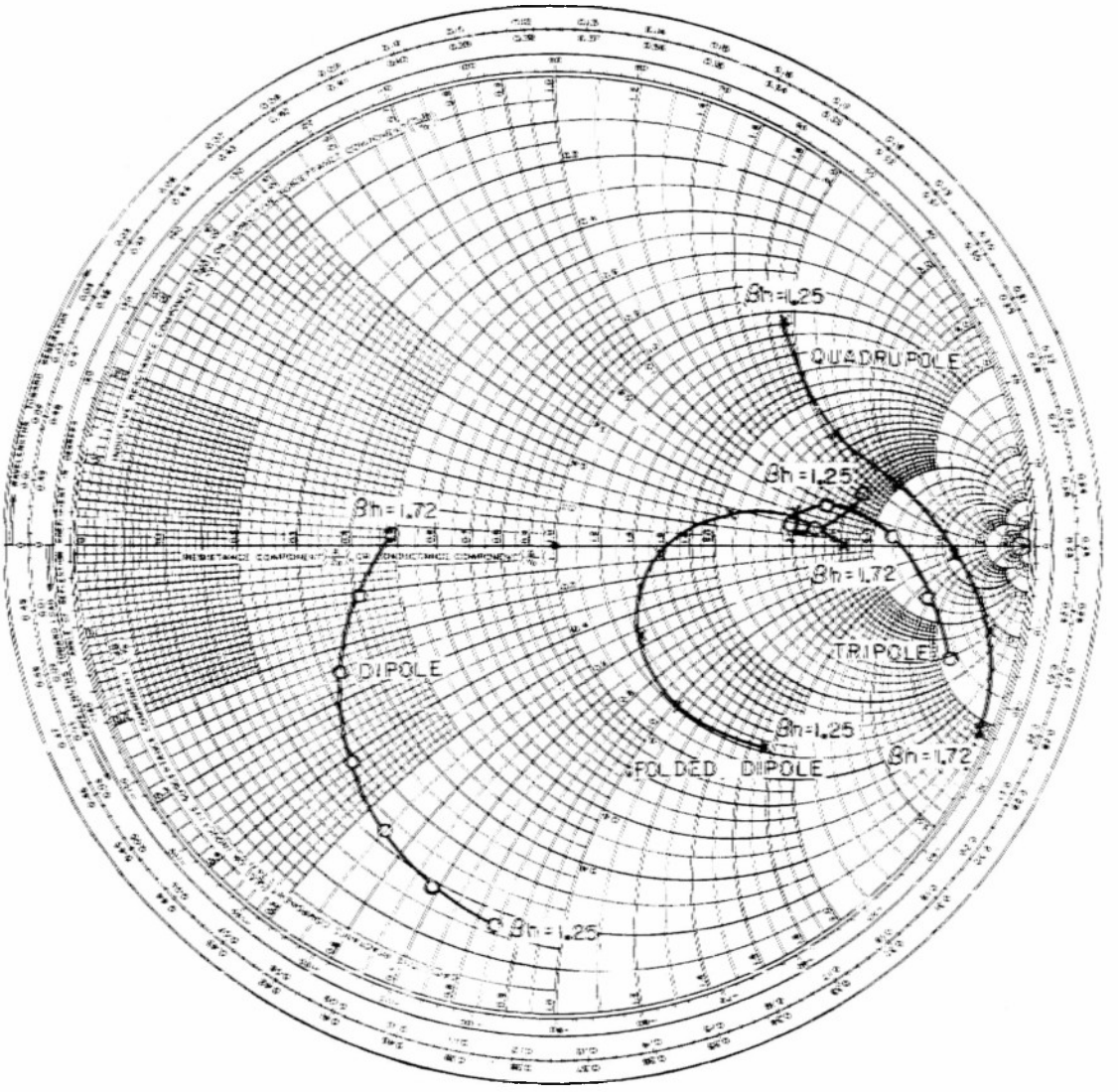

FIG. 3-4 CORRECTED ISOLATED ANTENNA IMPEDANCES

made with one setup at a time; consequently, the individual antennas had to be assembled and disassembled once for each measurement. Thus the more complicated the antenna structure, the less likely that the reassembled structure was identical to the first assembly, and connected in exactly the same position to the measuring apparatus. This is probably the major source of error, and is the reason for the fact that the folded quadrupole measurements were not duplicated. A third source of error arises from the ever-present contact difficulties at the point where the measured impedances must be plugged into the measuring apparatus. Actually, for a realistic calculation of percentage error, the measured differences should be compared to unity, the approximate normalized value of the standard resistive load; furthermore, it can be seen from the calculations that the susceptive part of the result is frequently computed from the difference between two values even greater than unity. This evaluation of error can more easily be justified by a comparison of the pairs of measured values of admittance plotted on the Smith Chart in Fig. 3-3.

Corrections as outlined in the preceding section have been applied to the average of each of the above measurements to determine the input impedance of each antenna at the plane of the antenna. The average values were chosen by drawing smooth curves through the pairs of measured values of g and b plotted as a function of antenna length, as well as on the Smith Chart of Fig. 3-3. Corrected results are plotted in Fig. 3-4, and given in Table 3-2 both with and without the image correction.

Table 3-1. Comparison of Measured Antenna Admittances

(Normalized at Reference Plane of Bridge Input Stub)

	h* cm	Impedance Bridge	Slotted Line
Simple	7.5	.1121 - j.2761	.1018 - j.2754
Dipole	8.0	.1312 - j.1756	.1260 - j.1730
	8.5	.1542 - j.0780	.1523 - j.0761
	9.0	.1839 + j.0163	.1814 + j.0165
	9.5	.2224 + j.1321	.2273 + j.1360
	10.0	.2667 + j.2358	.2776 + j.2404

*The overall length of each antenna is 2h + b, where b is the line spacing = 1/2 inch.

Table 3-1 (Cont'd).

	h cm	Impedance Bridge	Slotted Line
Simple Dipole	10.5	.3305 + j.3486	.3366 + j.3602
Folded	7.5	.6105 + j.6506	.6221 + j.5418
Dipole	8.0	1.0092 + j.4893	1.0476 + j.4836
(with λ/4	8.5	1.0868 + j.0448	1.1459 + j.0712
section)	9.0	.8578 - j.1424	.8769 - j.2197
	9.5	.5706 - j.2119	.6055 - j.2119
	10.0	.4477 - j.1026	.4603 - j.1341
	10.5	.3674 - j.0091	.3496 - j.0213
Folded	7.5	.2873 - j.0971	.2890 - j.1405
Tripole	8.0	.4162 - j.0747	.4227 - j.0754
(with λ/4	8.5	.4617 - j.0894	.4228 - j.1529
section)	9.0	.3440 - j.1049	.3796 - j.1125
	9.5	.2481 - j.0109	.2355 + j.0117
	10.0	.1853 + j.1323	.2133 + j.1030
	10.5	.1576 + j.2858	.1692 + j.2922
Folded	7.5	.2243 - j.4477	
Quadrupole	8.0	.2563 - j.3533	
(with λ/4	8.5	.2698 - j.2331	
section)	9.0	.1907 - j.1516	
	9.5	.1356 + j.0844	
	10.0	.0823 + j.2324	
	10.5	.0582 + j.5287	

Table 3-2. Corrected Antenna Impedances

βh	Average Normalized Measured Admittance	Antenna Input Z with Image (ohms)	Isolated Antenna Impedance (ohms)
Simple Dipole			
1.25	.1100 -j.2760	41.80 -j200.24	39.91 -j204.1
1.33	.1270 -j.1743	47.83 -j161.70	45.94 -j166.6
1.41	.1533 -j.0770	57.16 -j125.07	55.27 -j132.1

Table 3-2 (Cont'd).

βh	Average Normalized Measured Admittance	Antenna Input Z with Image (ohms)	Isolated Antenna Impedance (ohms)
1.49	.1827 +j.0164	67.58 -j 90.33	65.69 -j 99.8
1.57	.2248 +j.1340	82.19 -j 47.33	80.30 -j 59.6
1.64	.2750 +j.2380	99.54 -j 8.89	97.65 -j 25.1
1.72	.3336 +j.3325	119.72 +j 25.79	117.83 +j 6.1
Folded Dipole			
1.25	.6163 +j.6500	307.6 -j397.4	300.0 -j413.0
1.33	1.0284 +j.4865	301.8 -j224.5	294.2 -j244.1
1.41	1.1450 +j.0580	323.4 -j 99.67	315.8 -j127.7
1.49	.8673 -j.2197	390.1 +j 23.11	382.5 -j 14.9
1.57	.6050 -j.2119	517.2 +j124.5	509.6 +j 75.3
1.64	.4480 -j.1180	727.8 +j171.4	720.3 +j106.6
1.72	.3585 -j.0152	1003.0 +j 77.99	995.5 -j 0.8
Folded Tripole			
1.25	.2882 -j.0971	1027.5 +j417.6	1010.5 +j382.5
1.33	.4195 -j.0750	813.7 +j140.1	796.7 +j 96.0
1.41	.4600 -j.1050	725,7 +j143.2	708.6 +j 80.0
1.49	.3600 -j.1085	866.4 +j278.0	849.4 +j192.5
1.57	.2480 -j.0100	1417.8 +j229.8	1400.8 +j119.1
1.64	.1853 +j.1300	1532 -j772.9	1515 -j918.7
1.72	.1576 +j.2890	704.5 -j1174	687.5 -j1351
Folded Quadrupole			
1.25	.2243 -j.4477	281.4 +j523.8	251.1 +j461.4
1.33	.2563 -j.3533	419.6 +j558.9	389.4 +j480.5
1.41	.2550 -j.2331	657.4 +j626.0	627.2 +j514.0
1.49	.1907 -j.1050	1186.2 +j849.9	1156 +j697.9
1.57	.1300 +j.0500	2846 -j159.3	2816 -j356.1
1.64	.0900 +j.2325	792.7 -j1720	762.5 -j1980
1.72	.0582 +j.5287	91.97-j856.5	61.73-j1172

C. Unbalanced Terminations

One of the simplifying assumptions made in the theoretical analysis of the shielded two-wire hybrid junction in Technical Report No. 183 was that the terminations connected to the hybrid junction did not produce coupling between modes, which is generally true of symmetrical load structures. In all of the previous measurements, every effort was made to minimize coupling between modes, and in fact to suppress the unbalanced mode wherever possible. It was concluded from the theoretical analysis of the bridge operation that while unequal unbalanced reflections from the two load impedances would produce balanced components of voltage at the two detectors, these would be in phase and could be eliminated (or at least discriminated against) by connecting the two detector outputs together in phase opposition. This was not considered a major problem for the previous antenna measurements because the antennas were very nearly symmetrical and the driving voltage was almost purely of the balanced mode.

It would be interesting, therefore, to test the operation of the bridge with terminations which produce a large amount of coupling between modes. Theoretically, if properly adjusted, the bridge should respond only to balanced reflections from the loads. Tomiyasu (10) has made some slotted-line measurements on unbalanced antennas consisting of an extension of one wire of an open two-wire line beyond the other, over a ground screen 16 inches square. This is a convenient configuration for comparative measurements, since there will be very little coupling to the collinear image through the ground screen, and so the size of the ground screen will not have an appreciable effect. Accordingly, measurements of six unbalanced antennas were made on the bridge for different extensions "d" of one wire beyond the other, with the shorter wire extending 34.5 cm beyond the ground screen. The results of the measurements are given in Fig. 3-5, where the admittances are referred to the plane of the ground screen. These are compared with Tomiyasu's measured balanced reflection coefficients (Γ_{BB}) and are seen to agree very well.

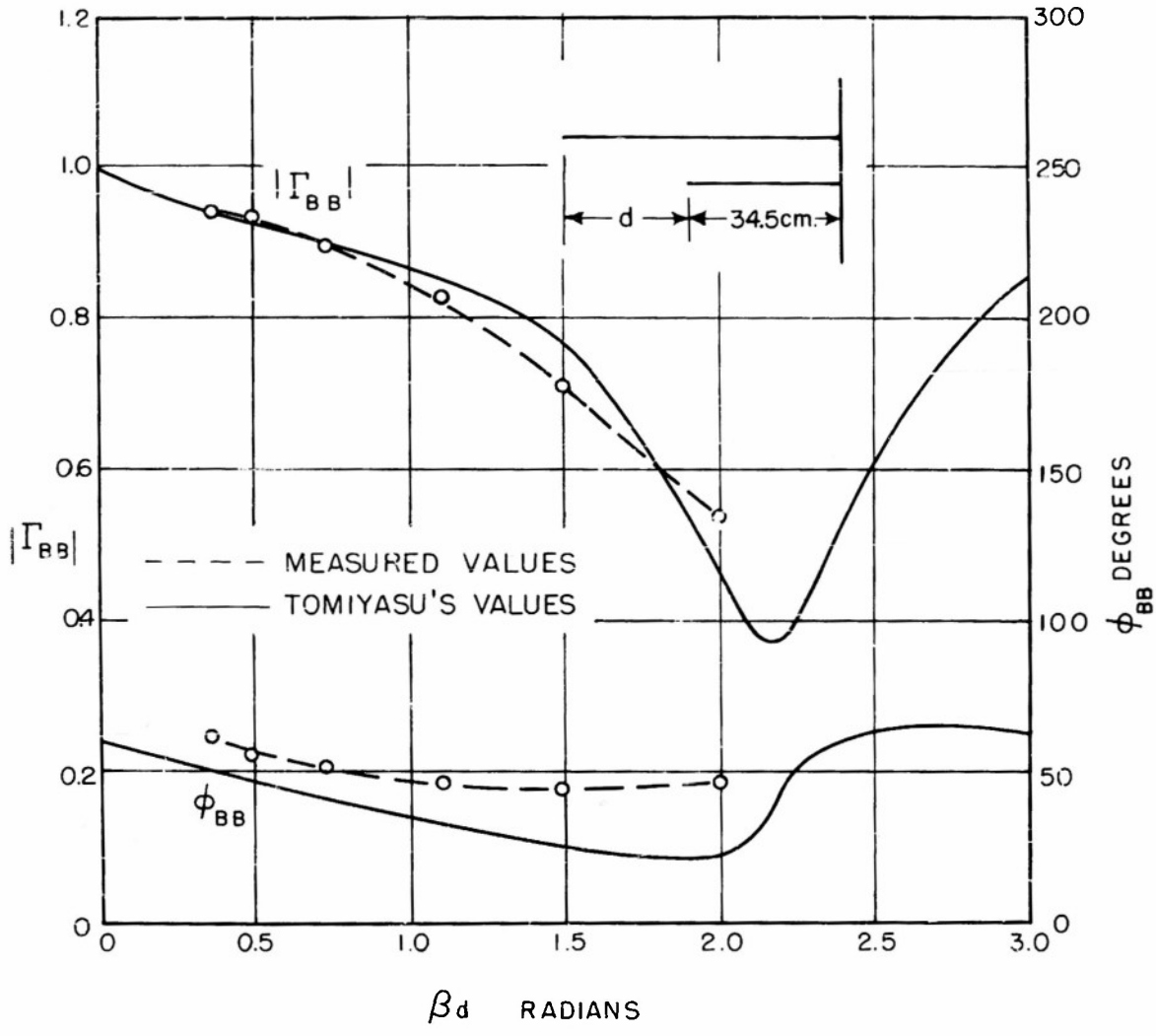

FIG. 3-5 Γ_{BB} OF UNBALANCED ANTENNAS

Table 3-3. Unbalanced Terminations

d cm	βd	g_{IN}	b_{IN}	$\lvert\Gamma_{BB}\rvert$	$\angle\Gamma_{BB}$ °
2.3	.356	.0393	-.5849	.940	61.2
3.15	.487	.0454	-.5169	.932	55.5
4.7	.727	.0694	-.4661	.896	51.1
7.1	1.100	.1184	-.4135	.826	46.1
9.6	1.484	.1960	-.3831	.710	44.0
12.75	1.97	.3610	-.3718	.535	46.5

Conclusions

A fair appraisal of the results of the balanced antenna measurements, with due regard for the existing experimental conditions, reasonably leads to the conclusion that bridge measurements of impedances which do not differ greatly in magnitude from the characteristic impedance of the transmission line used are accurate to the order of one or two per cent. Further measurements of identical impedances on both the bridge and the slotted line, with proper care to minimize contact difficulties, should serve to corroborate this figure. At the same time, it is evident that improved accuracy for other impedance ranges could be secured by variations in the impedance standard, either by changing the lumped resistive load and the stub spacing, or by utilizing a different type of standard. Measurements at other frequencies would require recalibration of the standard impedance, although calibration at a number of discrete frequencies should suffice to determine critical parameters of the standard impedance over a considerable frequency band.

The results of unbalanced antenna measurements indicate proper operation of the bridge with respect to cancellation of unbalanced reflections from primary-line terminations, with the conclusion that bridge measurements correspond to the balanced term of the reflection-coefficient matrix, Γ_{BB}. This condition was established by proper orientation and tuning of the two detectors, together with the use of equal-length lines to combine their outputs. Conversely, the factor Γ_{UU} could be measured by reversing one detector, providing an unbalanced input signal, and using an unbalanced stand-

ard impedance. A similar scheme would permit determination of the cross-coupling coefficients, indicating the versatility of this type of impedance-measuring device.

The shielded two-wire hybrid junction, which is the basic element of the impedance bridge described herein, may find a great many additional applications in the UHF region, similar to the waveguide magic-tee at microwave frequencies, such as a balanced mixer for low-noise figure UHF receivers, and a duplexer for transmission and reception with a single antenna.

Finally, it should be noted that the techniques employed to handle this case of two propagating modes may prove useful in other instances as well, such as for multi-mode propagation in waveguides.

Acknowledgment

The author wishes to express his appreciation to Professor R. W P. King for his invaluable advice and encouragement throughout this work, as well as to the other members of the Antenna Group who have helped by their criticism and suggestions.

Appendix A

Slotted-Line Polyfoam Corrections

If it is desired to correct slotted-line impedance measurements for the presence of a section of line with a dielectric constant slightly different from that of the remainder of the line, such as the polyfoam supporting section of the two-wire slotted line, the following procedures may be used. Call Z_a the impedance presented to the load end of the polyfoam section, and Z_b the impedance seen looking at Z_a through the polyfoam section of length x. Then,

$$Z_b = Z'_c \frac{Z_a + jZ'_c \tan \beta' x}{Z'_c + jZ_a \tan \beta' x} \qquad (A-1)$$

If β and Z_c are the phase constant and characteristic impedance, respectively, of the line with air dielectric, and β' and Z'_c similarly in polyfoam, then

$$\beta' = \sqrt{\epsilon}\,\beta \qquad \text{and} \qquad Z'_c = Z_c/\sqrt{\epsilon} \qquad (A-2)$$

where ϵ is the dielectric constant of polyfoam = 1.032. Thus for the general case Z_a and Z_b are related by a complex factor which depends on Z_a, so that no simple correction in the measured standing wave will suffice to account for the presence of the polyfoam, and it is easiest to utilize Eq.(A-1) directly in the impedance correction.

For the special case of very large standing-wave ratios, one can represent Z_a by a short-circuited line of length w, so that

$$Z_a = j Z_c \tan \beta w \qquad (A-3)$$

Since the polyfoam is nearly lossless, Z'_c can be considered real, and thus from (A-1) Z_b is imaginary and can be represented as

$$Z_b = j Z_c \tan \beta w' \qquad (A-4)$$

where w' is the effective distance between the output end of the polyfoam and the short circuit. If $Z'_c = Z_c$, then $w' = w + \sqrt{\epsilon}\, x$; and it is the departure from this value which can be accounted for by a correction of the observed position of the standing wave. Since this departure will be small, it can be written as

$$\beta\Delta = \beta(w'-w-\sqrt{\epsilon}x) = \tan\beta(w'-w-\sqrt{\epsilon}x) = \frac{\tan\beta w' - \tan\beta(w+\sqrt{\epsilon}x)}{1+\tan\beta w'\tan\beta(w+\sqrt{\epsilon}x)} \qquad (A-5)$$

But from Eqs. A-1, 2, 3, and 4.

$$\tan\beta w' = \frac{1}{\sqrt{\epsilon}}\left[\frac{\sqrt{\epsilon}\tan\beta w + \tan\beta\sqrt{\epsilon}x}{1-\sqrt{\epsilon}\tan\beta w\tan\beta\sqrt{\epsilon}x}\right] \qquad (A-6)$$

Combining Eqs. (A-5) and (A-6) gives

$$\beta\Delta = \frac{(\sqrt{\epsilon}-1)(\sqrt{\epsilon}\tan^2\beta w - 1)\tan\sqrt{\epsilon}\beta x + (\epsilon-1)\tan\beta w\tan^2\sqrt{\epsilon}\beta x}{\sqrt{\epsilon}(1+\tan^2\beta w) + (1+\epsilon\tan^2\beta w)\tan^2\sqrt{\epsilon}\beta x + (1-\epsilon)\tan\beta w\tan\sqrt{\epsilon}\beta x} \qquad (A-7)$$

For $\sqrt{\epsilon} = 1.016$, $x = 4.75''$, $\lambda = 16''$, $\tan\sqrt{\epsilon}\beta x = -2.9714$,

$$\beta\Delta = -.00477\,\frac{\tan^2\beta w - 5.849\tan\beta w - 0.983}{\tan^2\beta w + .00938\tan\beta w + 0.972} \qquad (A-8)$$

$$= .00477\,(\cos 2\beta w + 2.925\sin 2\beta w)$$

$$= .01475\sin(2\beta w + 18^{\circ}53')$$

In order to relate this correction factor to the scale reading "z" on the slotted line, measurements indicate that a short circuit on the slotted line at w = 10.109 cm causes a standing-wave minimum at z = 17.058 cm. From Eq. (A-8), $\beta\Delta = -.00456$, or $\Delta = -.030$ cm, so that the true position of the minimum (one wavelength from the short circuit) is z = 17.028 cm. Thus w = (27.137 - z) cm; substitution of this value for w in Eq. (A-8) permits calculation of the correction term Δ as a function of z, as plotted in Fig. A-1.

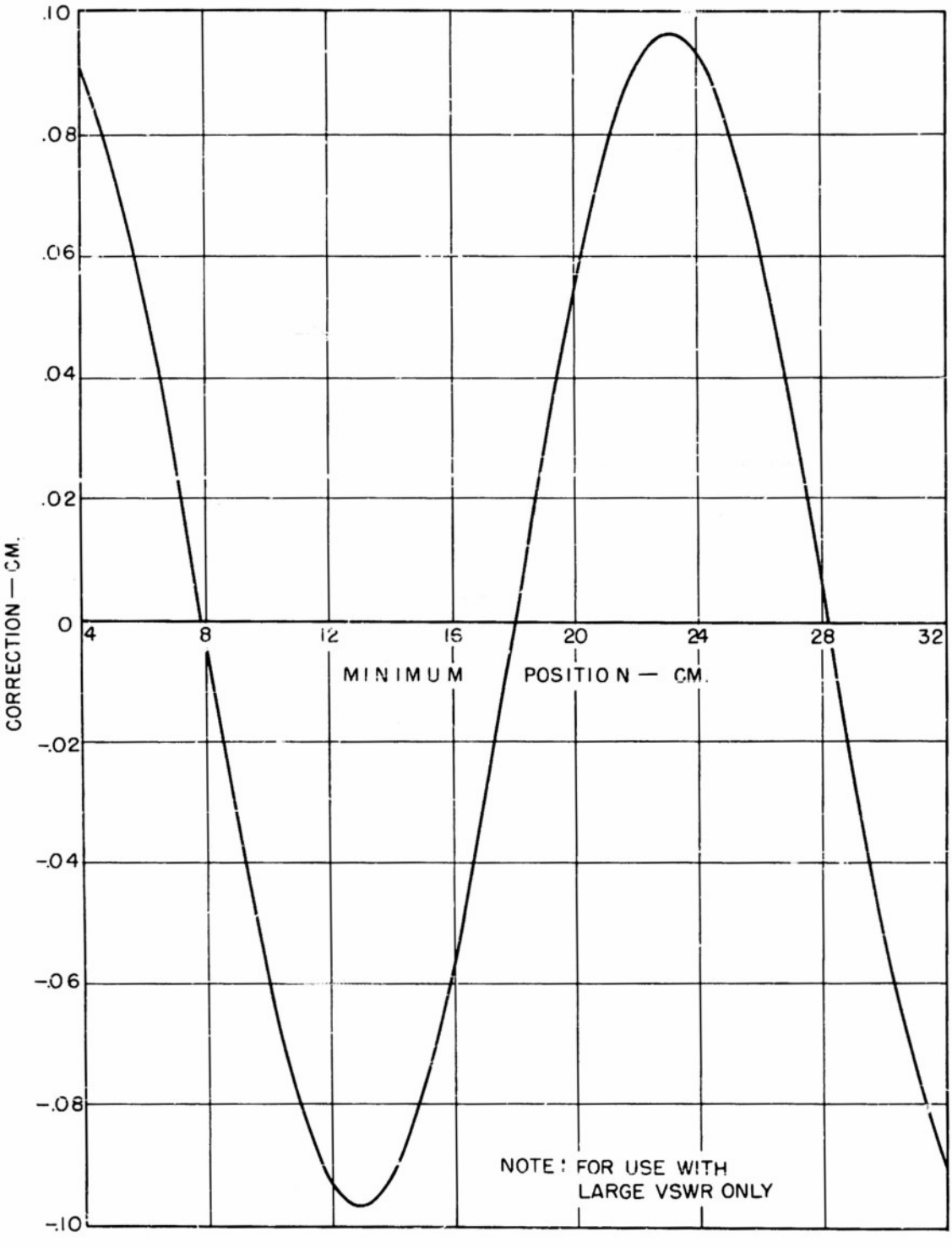

FIG. A-1 SLOTTED LINE CORRECTION CURVE

Appendix B

Characteristics of Measured Antennas

It was desired to measure impedances of simple dipoles and three types of folded dipoles with $\Omega \simeq 10$ for values of βh near $\pi/2$ (total antenna length = 2h). The factor Ω is given by

$$\Omega = 2 \ln \frac{2h}{a'} \qquad (B-1)$$

where a' is the effective radius of the antenna. For an array of n closely spaced parallel antenna elements each of radius a, spaced a distance b apart, a' is given by

$$a' = \sqrt[n]{a\, b^{n-1}} \qquad (B-2)$$

Since the same elements were to be used for each type of antenna, a value of b was calculated for each type to satisfy $\Omega \simeq 10$ for $\beta h = \pi/2$. For stability, it was decided to make all the antennas of 1/16-inch diameter brass rod, so the following values were used:

	a	b	Ω
Simple Dipole	.03125"	---	11.1
Folded Dipole	.03125"	.257"	9.0
Folded Tripole	.03125"	.180"	8.8
Folded Quadrupole	.03125"	.160"	8.6

Bibliography

1. Tomiyasu, K., "Problems of Measurement on Two-Wire Lines," J. Appl. Phys. 20, 892-896 (October, 1949); also Cruft Laboratory Technical Report No. 48, p. 61.

2. Morita, T., Sheingold, S., "A Coaxial Magic-T," Cruft Laboratory Technical Report No. 162 (November, 1952).

3. Deschamps, G.A., "Determination of Reflection Coefficients and Insertion Loss of a Waveguide Junction," J. Appl. Phys. 24, 1046-1050 (August, 1953).

4. Storer, J.E., Stein, S., Sheingold, L.S., "A Simple Graphical Analysis of Waveguide Junctions," Proc. I.R.E. 41, 1004-1013 (August, 1953); also Cruft Laboratory Technical Report No. 160.

5. Stein, S., Cruft Laboratory Technical Memorandum (to be published).

6. King, R.W.P., "Theory of Linear Antennas," Harvard University Press, Cambridge, Massachusetts, to be published 1954; part of which appears in J. Appl. Phys. 20, 832-850 (September, 1949).

7. Harrison, R.J., "Design Considerations for Directional Couplers," Massachusetts Institute of Technology Radiation Laboratory Report No. 724.

8. Cohn, S., "Principles of Transmission-Line Filter Design," Chapter 26 of Radio Research Laboratory, "VHF Techniques," Vol. II, McGraw-Hill, New York, 1947.

9. King, Ronold, "Transmission-Line Theory and its Applications," J. Appl. Phys. 14, 577-600 (November, 1943).

10. Tomiyasu, K., "Unbalanced Terminations on a Shielded-Pair Line," Cruft Laboratory Technical Report No. 86 (September, 1949).

11. Conley, P., "Impedance Measurements with Open-Wire Lines," J. Appl. Phys. 20, 1022-1026 (November, 1949); also Cruft Laboratory Technical Report No. 35.

12. King, R.W.P., Electromagnetic Engineering, Vol I, "Fundamentals," McGraw-Hill, New York, 1945, p. 477.

13. King, R., Harrison, C.W., Jr., "Mutual and Self-Impedance for Coupled Antennas," J. Appl. Phys. 15, 481-495 (June, 1944).

14. Tai, C.T., "The Theory of Coupled Antennas," Proc. I.R.E. 487-500 (April, 1948).

15. King, R., Middleton, D., "The Cylindrical Antenna; Current and Impedance," Q. Appl. Math. 3, 302-325 (January, 1946).

16. King, R.W.P., "Self and Mutual Impedances of Parallel Identical Antennas," Cruft Laboratory Technical Report No. 118.

17. Harrison, C.W., Jr., Doctoral Thesis, Harvard University, 1954.

DISTRIBUTION LIST

Technical Reports

2	Chief of Naval Research (427) Department of the Navy Washington 25, D. C.
1	Chief of Naval Research(460) Department of the Navy Washington 25, D. C.
1	Chief of Naval Research (421) Department of the Navy Washington 25, D. C.
6	Director (Code 2000) Naval Research Laboratory Washington 25, D. C.
2	Commanding Officer Office of Naval Research Branch Office 150 Causeway Street Boston, Massachusetts
1	Commanding Officer Office of Naval Research Branch Office 1000 Geary Street San Francisco 9, California
1	Commanding Officer Office of Naval Research Branch Office 1030 E. Green Street Pasadena, California
1	Commanding Officer Office of Naval Research Branch Office The John Crerar Library Building 86 East Randolph Street Chicago 1, Illinois
1	Commanding Officer Office of Naval Research Branch Office 346 Broadway New York 13, New York
3	Officer-in-Charge Office of Naval Research Navy No. 100 Fleet Post Office New York, N. Y.

1	Chief, Bureau of Ordnance (Re4) Navy Department Washington 25, D. C.
1	Chief, Bureau of Ordnance (AD-3) Navy Department Washington 25, D. C.
1	Chief, Bureau of Aeronautics (EL-1) Navy Department Washington 25, D. C.
2	Chief, Bureau of Ships (810) Navy Department Washington 25, D. C.
1	Chief of Naval Operations (Op-413) Navy Department Washington 25, D. C.
1	Chief of Naval Operations (Op-20) Navy Department Washington 25, D. C.
1	Chief of Naval Operations (Op-32) Navy Department Washington 25, D. C.
1	Director Naval Ordnance Laboratory White Oak, Maryland
2	Commander U. S. Naval Electronics Laboratory San Diego, California
1	Commander (AAEL) Naval Air Development Center Johnsville, Pennsylvania
1	Librarian U. S. Naval Post Graduate School Monterey, California
50	Director Signal Corps Engineering Laboratories Evans Signal Laboratory Supply Receiving Section Building No. 42 Belmar, New Jersey

3	Commanding General (RDRRP) Air Research and Development Command Post Office Box 1395 Baltimore 3, Maryland
2	Commanding General (RDDDE) Air Research and Development Command Post Office Box 1395 Baltimore 3, Maryland
1	Commanding General (WCRR) Wright Air Development Center Wright-Patterson Air Force Base, Ohio
1	Commanding General (WCRRH) Wright Air Development Center Wright-Patterson Air Force Base, Ohio
1	Commanding General (WCRE) Wright Air Development Center Wright-Patterson Air Force Base, Ohio
2	Commanding General (WCRET) Wright Air Development Center Wright-Patterson Air Force Base, Ohio
1	Commanding General (WCREO) Wright Air Development Center Wright-Patterson Air Force Base, Ohio
2	Commanding General (WCLR) Wright Air Development Center Wright-Patterson Air Force Base, Ohio
1	Commanding General (WCLRR) Wright Air Development Center Wright-Patterson Air Force Base, Ohio
2	Technical Library Commanding General Wright Air Development Center Wright-Patterson Air Force Base, Ohio
1	Commanding General (RCREC-4C) Rome Air Development Center Griffiss Air Force Base Rome, New York
1	Commanding General (RCR) Rome Air Development Center Griffiss Air Force Base Rome, New York

2	Commanding General (RCRW) Rome Air Development Center Griffiss Air Force Base Rome, New York
6	Commanding General (CRR) Air Force Cambridge Research Center 230 Albany Street Cambridge 39, Massachusetts
1	Commanding General Technical Library Air Force Cambridge Research Center 230 Albany Street Cambridge 39, Massachusetts
2	Director Air University Library Maxwell Air Force Base, Alabama
1	Commander Patrick Air Force Base Cocoa, Florida
2	Chief, Western Division Air Research and Development Command P. O. Box 2035 Pasadena, California
1	Chief, European Office Air Research and Development Command Shell Building 60 Rue Ravenstein Brussels, Belgium
1	U. S. Coast Guard (EEE) 1300 E Street, N. W. Washington, D. C.
1	Assistant Secretary of Defense (Research and Development) Research and Development Board Department of Defense Washington 25, D. C.
5	Armed Services Technical Information Agency Document Service Center Knott Building Dayton 2, Ohio

1	Director Division 14, Librarian National Bureau of Standards Connecticut Avenue and Van Ness St., N. W.
1	Director Division 14, Librarian National Bureau of Standards Connecticut Avenue and Van Ness St., N. W.
1	Office of Technical Services Department of Commerce Washington 25, D. C.
1	Commanding Officer and Director U. S. Underwater Sound Laboratory New London, Connecticut
1	Federal Telecommunications Laboratories, Inc. Technical Library 500 Washington Avenue Nutley, New Jersey
1	Librarian Radio Corporation of America RCA Laboratories Princeton, New Jersey
1	Sperry Gyroscope Company Engineering Librarian Great Neck, L. I., New York
1	Watson Laboratories Library Red Bank, New Jersey
1	Professor E. Weber Polytechnic Institute of Brooklyn 99 Livingston Street Brooklyn 2, New York
1	University of California Department of Electrical Engineering Berkeley, California
1	Dr. E. T. Booth Hudson Laboratories 145 Palisade Street Dobbs Ferry, New York
1	Cornell University Department of Electrical Engineering Ithaca, New York

1	University of Illinois Department of Electrical Engineering Urbana, Illinois
1	Johns Hopkins University Applied Physics Laboratory Silver Spring, Maryland
1	Professor A. von Hippel Massachusetts Institute of Technology Research Laboratory for Insulation Research Cambridge, Massachusetts
1	Director Lincoln Laboratory Massachusetts Institute of Technology Cambridge 39, Massachusetts
1	Signal Corps Liaison Office Massachusetts Institute of Technology Cambridge 39, Massachusetts
1	Mr. Hewitt Massachusetts Institute of Technology Document Room Research Laboratory of Electronics Cambridge, Massachusetts
1	Stanford University Electronics Research Laboratory Stanford, California
1	Professor A. W. Straiton University of Texas Department of Electrical Engineering Austin 12, Texas
1	Yale University Department of Electrical Engineering New Haven, Connecticut
1	Mr. James F. Trosch, Administrative Aide Columbia Radiation Laboratory Columbia University 538 West 120th Street New York 27, N. Y.
1	Dr. J.V.N. Granger Stanford Research Institute Stanford, California